



BELBaR D5.1

DESCRIPTION OF CONCEPTUAL MODELS AND THE RELATED MATHEMATICAL MODELS TO SUPPORT TREATMENT OF COLLOIDS RELATED ISSUES IN THE SAFETY CASE

June 2012

Ivars Neretnieks, Luis Moreno, Longcheng Liu

Royal Institute of Technology
School of Chemical Science and Engineering
SWEDEN

Markus Olin, Veli-Matti Pulkkanen

VTT
FINLAND

Thorsten Schaefer, Florian Huber

Karlsruhe Institute of Technology (KIT)
Institute for Nuclear Waste Disposal (INE)
GERMANY

Kari Koskinen (ed.)

Posiva
FINLAND

The research leading to these results has received funding from the European Atomic Energy Community's Seventh Framework Programme (FP7/2007-2011) under grant agreement n° 295487.

1	Definition of the system	4
2	System conceptualization	4
2.1	Erosion of bentonite	4
2.2	Transport of bentonite colloids	5
3	Models and the related aspects on implementation	5
3.1	Erosion of bentonite - baseline model by KTH	5
3.1.1	Introduction and background	5
3.1.2	Bentonite gel/sol properties	6
3.1.3	Conceptual model(s) of bentonite erosion	7
3.1.3.1	Earlier modelling	7
3.1.3.2	Underlying concepts and mechanisms	8
3.1.3.3	Conceptual picture of bentonite erosion into a fracture	11
3.1.4	Viscosity of smectite gel/sol	15
3.1.5	Forces on and between smectite particles	17
3.1.5.1	Overview	17
3.1.5.2	Forces involved	18
3.1.5.3	Balancing the forces	22
3.1.6	Dynamic model for gel/sol expansion	24
3.1.6.1	Mathematical model for bentonite expansion in a fracture and release of colloids	25
3.1.6.2	An example of simulation results	26
3.2	Erosion of bentonite - modifications of baseline model by VTT	28
3.2.1	Introduction	28
3.2.2	The modifications implemented	28
3.3	Transport of bentonite colloids	31
3.3.1	Conceptual models	31
3.3.1.1	Interactions with the stationary phase	31
3.3.1.2	Heterogeneity of the domain	32
3.3.2	Numerical implementation	32
	Notation	33
	References	34

1 Definition of the system

Colloids related issues are relevant in the safety cases of nuclear waste disposal in crystalline rocks. More specifically, since natural colloids concentrations in typical repository conditions are negligible the most outstanding potential for colloids are in the colloids generated from clay and cementitious components. An example of such concept is KBS-3.

These colloids are relevant from the point of view of probability of colloids mediated radionuclide transport and as a consequence of inappropriate degeneration of engineered barrier system. Thus preeminent changes in the properties of the system include

- decrease of clay density or the density of cementitious material at and near their interface with groundwater with respect to the initial causing further changes in some performance indicators like hydraulic conductivities of components in question,
- increase of the thickness of the diffusional barrier at the locations in which fractures intersect clay components,
- increase in hydraulic conductivity at the locations in which fractures intersect cementitious components, and
- increase in the amount of colloids available as carriers for radionuclides.

In this connection the focus is in clay colloids and cement derived colloids are omitted.

2 System conceptualization

2.1 Erosion of bentonite

Currently the system is described in terms of solids content distribution within clay components and hydraulic and mechanical properties depending on it. Initial solids content distribution has been shown to meet the requirements (e.g. SKB 2011, TR 11-01) such that adequate swelling pressures and hydraulic conductivities are reached. Porewater composition of clays will change should there be changes in geochemical conditions in the repository. Decrease in groundwater ionic strength is of utmost importance in this connection. The rate of change of porewater composition is limited by diffusional transport of porewater solutes to and from groundwater. Changes in porewater composition influence solids content and hydraulic and mechanical properties. These couplings are illustrated in Figure 2.1.

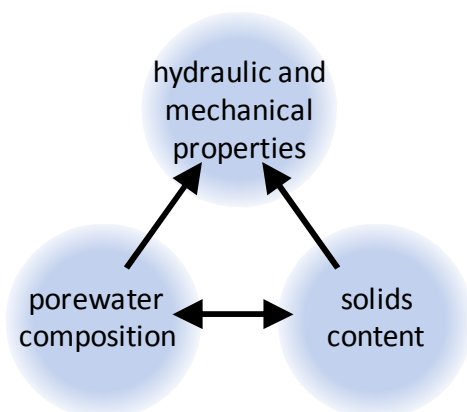


Figure 2.1. Illustration of couplings between solids content of clay, clay porewater composition, and clay's hydraulic and mechanical properties.

Moreover, the solids lost from clay component are considered primarily as colloids fed into the groundwater in the fracture intersecting the part of repository in question.

Aspects not considered in the current conceptual models and with uncertain contributions are the effects of

- divalent cations in porewater and
- all fracture minerals available at different host rocks.

An account of measurable characteristics and features with respect to which advances could be expected is presented in deliverable D1.1.

2.2 Transport of bentonite colloids

Currently the transport of colloidal phases is usually described in terms of models based on the advection-dispersion equation (Sen and Khilar, 2006). The source terms embedded describe the interaction with the stationary phase either as equilibrium or as a non-equilibrium process.

An account of measurable characteristics and features with respect to which advances could be expected is presented in deliverable D1.1.

3 Models and the related aspects on implementation

3.1 Erosion of bentonite - baseline model by KTH

3.1.1 Introduction and background

In Finland and Sweden, repositories for spent nuclear fuel are planned to be located at about 500 m depth in sparsely fractured granitic rock. The spent fuel is emplaced in copper canisters. The canisters are surrounded by highly compacted bentonite, which swells as water from the rock intrudes and saturates it. The integrity of the canister is one of the important features of the repository design. A main function for the buffer is to ensure that the intrusion of corrosive agents is kept low. The hydraulic conductivity of the saturated bentonite is so low that the pore water is effectively stagnant and dissolved constituents, including any corrosive agents, migrate very slowly through the buffer only by molecular diffusion. Should a large portion of the buffer be lost the protective function would be impaired.

The compact bentonite buffer consists of mostly colloidal sized smectite clay particles that exert a very large swelling pressure. In dilute water the small particles can swell out into fractures that intersect the deposition hole and thus some buffer may be lost. Furthermore, in waters with low ionic strength the smectite particles can solubilize, i.e. form a stable sol that can be carried away by the seeping water in the fracture. Low ionic strength waters below the critical coagulation concentration (CCC) may intrude a repository. At higher ionic strengths above the CCC sols will not form as the gel becomes cohesive at some volume fraction of smectite. Expansion of the gel into the fracture may still occur as long as the gel is still expansive. It is also conceivable that very high water velocities could shear off gel even from a cohesive gel. It is also conceivable that under some conditions gravity could help dislodge particles or agglomerates from the gel. These and other effects must be considered.

Properties of bentonite clays

Bentonites consists mostly of montmorillonite typically contain tens of percent of accessory minerals. Common accessory minerals are quartz, feldspar, calcite and gypsum. Montmorillonite is a member of the smectite family. It is a 2:1 clay built up of a central octahedral layer sandwiched by two tetrahedral layers, as illustrated schematically in 3.1. The octahedral layer consists mostly of aluminium oxide and the tetrahedral layer of mostly silicon oxide (van Olphen 1977, Bergaya et al. 2006). The particles are thin

irregular plate-shaped sheets with diameters ranging from a few tens of nm to several hundred nm. In the octahedral layer the trivalent aluminium in some locations is substituted for magnesium, iron or some other divalent metal. In the tetrahedral layer the silica is occasionally substituted for aluminium as is seen in Figure 3.1. This generates a negative surplus charge on the order of one charge equivalent per kg. This is compensated by cations residing at the outer surfaces of the smectite sheets. When the clay takes up water, the charge compensating cations will stay near the surface of the sheets, forming a thin diffuse layer with a high concentration of cations nearest the surface and a decreasing cation concentration with increasing distance from the surface. The diffuse layers of nearby sheets repel each other. These repulsion forces cause a strong swelling pressure when the particles are close to each other in the compacted clay.

The most common charge compensating cations are sodium and calcium, although potassium and magnesium are also found present. When the dominating cation is sodium or calcium the clay is often called sodium bentonite and calcium bentonite respectively. Sodium and calcium bentonites have somewhat different swelling properties when wetted, and also have different tendencies to disperse in water. The charge compensating cations are only bound to the surface of the sheets by electrostatic forces. They can readily be ion exchanged for other cations. This can be expressed as the cation exchange capacity, CEC. The CEC can be considerably different in bentonites from different locations. Values ranging from 0.27 to 0.87 equivalents per kg are reported (Karnland et al. 2006).

An originally sodium rich bentonite will exchange the sodium for calcium when exposed to a calcium rich water and vice versa. This can impact the evolution of the swelling and other properties of the clay.

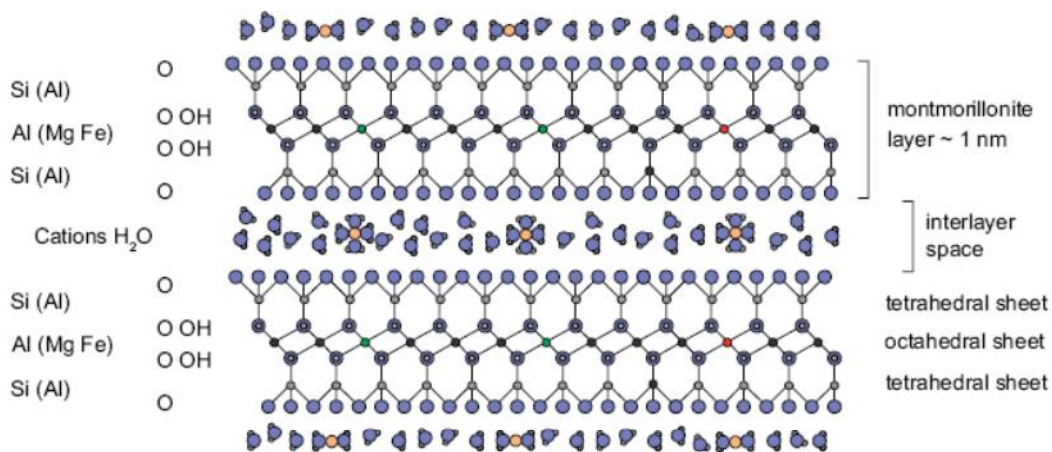


Figure 3.1. Structure of montmorillonite

The accessory mineral particles are on average much larger than the smectite particles and have much smaller surplus charge. They influence the swelling properties of the clay and cannot move far into the smallest rock fractures into which swelling clay will expand because the apertures of these fractures are smaller than the mean particle size of the detritus. This potential clogging of the rock fractures may slow down or hinder erosion.

3.1.2 Bentonite gel/sol properties

Compacted bentonite has a very high swelling pressure when wetted. Several tens of MPa are typically found for a dry density of 1700 kg/m³. A buffer with this density has porosity around 37%. If the bentonite is allowed to swell the density and the swelling pressures decreases. Further swelling decreases the volume fraction of bentonite and the swelling pressure becomes increasingly lower. A sodium exchanged Wyoming bentonite at 80% porosity (20% volume fraction of bentonite) still has a swelling pressure in the range 0.03 to 0.3 MPa depending on the water ionic strength. Except for very high compaction the higher the ionic strength, the lower is the swelling pressure. Swelling can stop entirely, at a given volume fraction, when the

ionic strength in the pore water is above the critical coagulation concentration, CCC. It should be noted that below the CCC, sodium dominated smectite would expand “forever” eventually filling up all available water volume unless held back by gravity. Horizontal swelling will not be influenced by gravity and downward expansion will be aided by gravity. The gel turns into a sol in which the repulsion forces between particles hinder them from recombining. During these conditions colloids are formed and the sol can be transported away by the water seeping in the fractures. This will cause erosion of the buffer. Above the CCC compacted bentonite will swell to a certain extent but will not release colloidal particles by thermal (Brownian) movement. Sodium dominated bentonites swell much more than calcium dominated ones, which are less prone to release colloids.

Bentonite clays exhibit strongly non-linear viscous properties. They can appear solid for stresses below a critical limit, called yield stress fluids. Thixotropy is another prominent feature of bentonite gels. Even at moderately low volume fractions the expanding gel has a very high viscosity. It is expected that the gel/sol viscous properties can play an important role for the erosion of the bentonite because as the gel expands into the seeping water in the fracture its viscosity will decrease and it will flow, albeit with lower velocity than water without particles. Thus the influence of both particle concentration and ionic strength of the water must be understood.

The flat smectite sheets are very thin consisting of essentially three layers of aluminium and silicon oxide groups as shown in Figure 3.1. The sheets are about 1 nm thick. In the other two dimensions the sizes range from 50 to few hundred nm. The accessory minerals are much larger but typically less than 0.1 mm.

3.1.3 Conceptual model(s) of bentonite erosion

3.1.3.1 Earlier modelling

Several studies have been made on erosion of bentonites. Pusch (1983, 1999, and 2007) discussed stability of bentonite gels in crystalline rock. Boisson (1989) addressed the possible erosion of bentonite by flowing water. Kanno and Wakamatsu (1991) and Kanno et al, (1999) performed experiments on bentonite erosion. Sjöblom et al. (1999) studied erosion in connection with possible retrieval of canisters. Grindrod et al. (1999) considered mechanical erosion and colloid formation by flowing groundwater. Kurosawa et al (1999) studied erosion properties and dispersion-flocculation behaviour of bentonite particles. Verbeke et al. (1997) addressed the long-term behaviour of buffer materials in geologic repositories for high-level wastes. Tanai and Matsumoto, (2007): studied the extrusion behaviour of buffer material into fractures using an X-ray CT method. These studies mostly discuss physical erosion mechanisms. None of them address the details of chemical and surface chemical process in depth.

SKB managed the so-called erosion project during 2006 to 2009 in which a number of experimental and theoretical studies were performed. The main reports summarising this work are Neretnieks et al (2009) where the emphasis is on model development and Birgersson et al. (2009) with emphasis on experiments.

Liu and Neretnieks (2006) seem to be the first to quantitatively address the role of chemistry that may influence the rate of colloid generation and the resulting erosion. Liu (2010) and Liu et al. (2009a) devised a dynamic model for pure smectite swelling and colloid release that accounts for competing attractive and repulsive forces between the smectite particles as well as on them by thermal movement (Brownian motion) and gravity. The model accounts for the influence of monovalent cations but not for divalent ions such as calcium. The model was validated by experiments of compacted smectite pellets swelling in distilled and low ionic strength waters and experiment on penetration through fine pore filters. The model was also used to derive a new method to determine the CCC, which gave about two orders of magnitude better results than the conventional DLVO model, (Liu 2011). The results agree well with observed values.

A gel viscosity model accounting for the influence of sodium concentration was devised based on published experimental results Liu (2011).

The dynamic model together with the viscosity model was used to simulate the rate of expansion of smectite into a fracture with flowing water. The expanding viscous gel can flow and release particles at the gel/sol/water interface. The gel/sol is carried downstream. The rate of loss of smectite and the distance to which the gel expands into the fracture was modelled for some cases relevant to the KBS-3 repository concept (Moreno et al. 2011). In this model the simultaneous diffusion of sodium from the buffer in the deposition hole towards and into the water seeping past the gel/sol/water interfaces also was accounted for. Below some more details of the concepts underlying this model are given.

3.1.3.2 Underlying concepts and mechanisms

Gel/sol behaviour and expansion

When the water in contact with the clay contains dissolved salts in a concentration above the CCC the clay particles swell to a certain volume fraction but not more. At this point the gel is cohesive and will not release particles spontaneously. Swollen clay that has penetrated some distance into the fracture mouth can be sheared and release gel particles if shear forces are higher than the cohesive forces in the gel. It is not likely that the cohesive gel will be sheared off by the flowing water at the possible water velocities.

Should very fresh water flow in the fractures, the salt initially in the pore water in the gel will diffuse out into the water and be carried away. The ion concentration will drop below the CCC. Then the particles will no longer be attracted to each other, on the contrary, repulsive forces will dominate and force the gel to expand. This expansion strives to force the particles as far as possible from each other. The outermost particles move into the flowing water, which carries them away.

Under saturated conditions the gel *mass itself does not need to move* for gel “expansion” to take place. In the expanding gel the forces between the smectite particles force them to distance themselves from each other. The rate of movement is restrained by the friction of the particles against the water surrounding them. When a particle moves from one position to another its vacated place is taken by exactly the same volume of water. There is thus no net movement of gel volume. The particles and water just change place. The phenomenon can be compared to when two different liquids that are suddenly placed in contact with each other. The molecules from liquid A diffuse into liquid B. The B-molecules diffuse in the other direction into liquid A. The bulk of the liquid does not move at all.

At high smectite concentration in the gel it is expected that steric effects hinder the smectite sheets to move independent of each other and that also the presence of e.g. fracture surfaces may influence the gel expansion.

Should fresh water flow over long periods; considerable amounts of clay could be washed away, at least in the fractures with high flowrates. The particles could form a stable colloidal suspension in the low salinity waters and could be carried very long distances without being filtered or clog the fracture network. As the particles have an inherent negative charge and the minerals in the fractured rock also are mostly neutral or negatively charged, the smectite particles will not be attracted to them. The little fraction of the surface that can have a positive charge may bind some particles but when these sites are filled no more particles will stick to the surfaces. Thus filtering of the colloids in the fractures is not expected to slow down erosion markedly unless the fractures contain much small particles that can form a physical filter.

In the gel the main forces acting on the particles are gravitation, buoyancy, diffusion, electrical diffuse double layer repulsive forces (DDL) and van der Waals (vdW) attractive forces. Particle movement caused by these forces are balanced by friction against the water. Only the DDL forces are influenced by the water composition to an appreciable degree. In water with ionic strength below the CCC, the DDL forces dominate over the vdW forces and the particles repel each other at all distances. At high particle concentrations, as in compacted clay, the forces are very large. The clay expands and the rate of expansion is governed by the balance of net repulsion forces and the friction forces of the particles *in the water*.

Friction of the gel, containing only montmorillonite particles and water, against the *fracture walls* seems not to influence or limit gel expansion. This can be understood by the fact that there is no net gel flow relative to the walls of the container so there is no friction against the walls. A smectite particle that moves will be replaced by the same water volume moving in the other direction. The smectite particles can be compared to very large molecules and they also move as such by the thermal forces (Brownian movement). This is supported by experiments with filters with very small pores where it is found that a 2 mm thick filter with pore sizes of 2 μm allows smectite particles to penetrate nearly as rapidly as through 10 μm filters (Birgersson et al. 2009, Neretnieks et al. 2009). Should wall friction between the gel/sol and pore walls, as for a fluid flowing through a porous medium have played a role, the finer filter should have slowed down the flow by a factor 25. This is because the flowrate in each pore is proportional to the pore diameter to the 4th power and the total number of pores is inversely proportional to the diameter to the 2nd power. This gives the flowrate per cross section area of the filter proportional to the diameter to the 2nd power.

Ion exchange and influence of calcium and other divalent ions

The above description of gel/sol behaviour applies best to smectites in which monovalent ions such as sodium dominate in the water and in the diffuse double layer. Then the individual sheets tend to separate and the colloid particles consist of one sheet. CCC is then in the range 20-100 mM. When the pore water has essentially only divalent ions such as calcium or magnesium these also will be present in the diffuse double layer.

Actually the term porewater is not well defined because the diffuse double layer containing the charge compensating cations has a high concentration nearest to the surface and the concentration gradually falls off with distance. When both monovalent and divalent ions are present in the water the ions in water nearest the surface have a different fraction of di/monovalent ions than in the water further from the surface. This implies that on the average the composition of the amount of counterions needed to compensate for the smectite charge is different from the water at large distance from the surface.

Divalent ions are much preferred in the diffuse layer compared to monovalent ions. At low concentration in the surrounding water (at large distances from the surface) even a small fraction of calcium can generate a high fraction of calcium in the charge diffuse layer. It has been found that for approximately up to 90% calcium in the diffuse layer the smectite behaves much like a sodium smectite. At larger calcium fractions the smectite particles form stacks of typically 5 -10 to perhaps 20 sheets. The CCC for calcium smectite is 2-4 mM (Birgersson et al 2009). The stacks repel each other with forces comparable to those for the individual sheets in sodium-dominated systems. This manifest itself in that the swelling pressure of highly compacted calcium bentonite is comparable to that of sodium bentonite but that calcium bentonite stops expanding at much higher volume fraction smectite than its sodium counterpart. Calcium dominated bentonites are not expected to release colloidal particles as easily and the particles are expected to be larger because of the stack formation.

At low ion concentrations, even in dilute gels, the amount of cations in the diffuse layer makes up the by far largest fraction of all cations in the gel. Ion exchange equilibria thus are expected to strongly impact on the gel/sol properties. The cations in the diffuse layer are mobile and may dominate the rate of cation diffusion in the gel (Neretnieks et al. 2009). This does not seem to have been accounted for in many modelling studies of ion exchange in bentonite buffers.

Friction in fractures

Friction of the *incompressible* gel, containing only smectite particles and water, against the *fracture walls* does not to hinder smectite particle migration from a closed volume into a fracture.

However, wall friction may be limit *flow* of gel into fractures. Figure 3.2 illustrates a situation where the gel is enclosed in a vessel on all sides. One wall is in contact with a thin slit (fracture) filled with water. The gel exerts a strong swelling pressure on all walls of the vessel. This pressure cannot force any of the

incompressible gel to flow into fracture because if a tiny volume of gel mass were to be pressed out into the fracture the same volume of water would have to intrude to replace the vacated volume. Water can only intrude through the fracture and has to pass the smectite particles there, which occurs by the mutual exchange of water and smectite in the “expanding” gel in the fracture. This is governed by the force balance described above.

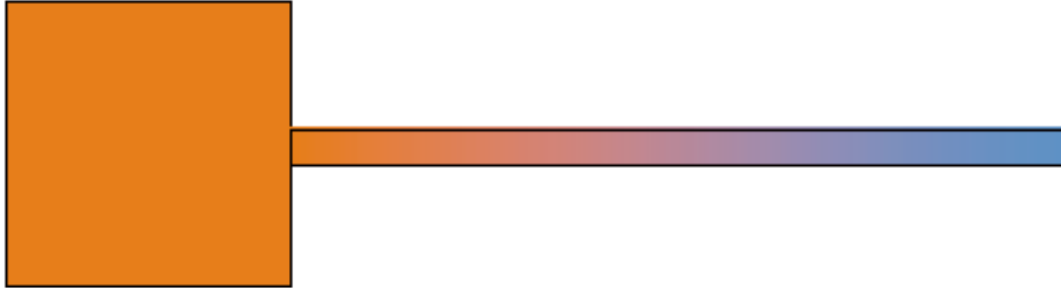


Figure 3.2. *The walls of the vessel are impervious to water and smectite. The gel is fully water saturated and the fracture is filled with water.*

Should any of the walls of the vessel allow water to enter the vessel, the situation would be different. Then the swelling pressure would expand the gel in the vessel and force the gel to flow into the fracture in addition to the gel swelling caused by the internal forces in the fracture. This flow will be counteracted by friction against the walls. It was shown in Birgersson et al. (2009) that the mass of gel can only expand very short distances in narrow fractures due to wall friction.

Gravity and Brownian diffusion have a negligible impact at high particle concentrations and ionic strengths but can become important at low concentrations. Below the CCC the gel continues to expand by the DDL forces until these are so weak that thermal (Brownian) motion of the particles becomes more important to further dilute the system, which now has turned from a gel into a sol. Gravity then also starts to play a role. In upward expansion, gravity pulls back the particles and in a downward expansion it helps the particles to move. Horizontal expansion where gravity has no impact would allow the sol to expand into all available water volume.

The gel is thixotropic and behaves as a pseudoplastic fluid. In a range of particle concentrations around one to a few volume percent the gel is more viscous when at rest and less viscous when subjected to shear. A rested gel will need a larger shear force to set it in motion and to shear off particles at the gel/water interface. However, once the gel has been set in motion it will flow more easily.

The gel does not flow like a Newtonian fluid such as water but deforms slowly when subjected to a shear force. Sometimes a minimum shear force, the yield stress, is needed to start deforming it. The gel behaves like a Bingham body or fluid. At shear stresses larger than the yield stress it flows nearly like a Newtonian fluid. Often in practice there is not so clear minimum shear stress but more gradual decrease in viscosity with increasing shear rate. As the viscosity is the ratio between shear stress and shear rate, the viscosity seems to decrease as more force is applied. The higher the particle concentration is the more nonlinear these effects are.

This has an important impact on the erosion. At particle concentrations of 2-5 % volume fraction or more, the viscosity of the gel at low shear forces is several orders of magnitude higher than that of water. With decreasing particle concentration the viscosity decreases and approaches that of water. The dilute gel/sol flowing in the fracture flows more slowly than water. The whole gel, if the stress is larger than the yield stress, can be set in motion. In the repository situation it is gradually replaced by more swelling gel from the deposition hole.

Above the CCC the gel expands to a point where the vdW attractive forces become equal to the DDL forces, which have decreased with distance between particles. When this point is reached, the gel expansion stops and particles that try to escape by thermal motion are pulled back. Particles are not spontaneously released and the gel is called a *cohesive gel* at this point. However, up to the volume fracture where the DDL and vdW forces balance (the balance point) the DDL forces dominate and the gel *is expansive* also when above the CCC. The gel will therefore continue to expand until all the gel has attained the volume fraction that corresponds to that at the CCC.

A very sharp boundary between gel and water develops at the balance point. Gravity may also act as a force that can balance the repulsive DDL force. It should be noted, that in most experiments using visual observations to determine the CCC, gravity could have played a role to restrain colloid dispersion to a dilute sol. The gel may well be expansive in the sense that if gravity would not restrain the expansion e.g. in a horizontal fracture the gel below CCC would expand forever forming an increasingly dilute sol.

3.1.3.3 *Conceptual picture of bentonite erosion into a fracture*

Figure 3.3 shows a fracture intersecting the canister deposition hole, which is filled with compacted bentonite. The bentonite, when wetted, swells out into the fracture. It has a very high swelling pressure when highly compacted but the swelling pressure decreases with decreasing bentonite density. The smectite particles are pulled and pushed into the water that seeps in the fracture by the different forces acting on the particles. If the pore water is below the CCC the particles at the bentonite/water interface can diffuse into the water and be carried away. There is also a region where the gel/sol has so low a particle concentration that it is little more viscous than water and can flow away. The loss of particles is thus influenced both by particle diffusion and by advective flow of the dilute gel/sol. For both mechanisms, the flowrate of water and gel in the fracture will influence the total rate of loss.

The water composition strongly influences the DDL forces but has a very weak or negligible influence on the other forces. The viscosity of the dilute gel increases with decreasing ionic strength. The CCC determines when the smectite particles can be released to the water in the form of colloids or when they still will be held together by the attractive vdW forces. It can be used to set up the borderline between a cohesive and an expansive gel. If the gel at the gel/water interface is cohesive, it can behave like a pseudoplastic or Bingham body and may not start to flow or allow shearing off of gel by the small shear forces the seeping water in the fractures can generate.

The water composition in the deep groundwaters at repository depth is normally above the CCC and very little release of colloids is expected. It is also not expected that the cohesive gel can be sheared away at any of the expected water velocities. However, if fresh water were to intrude, the water composition at the gel/water interface could decrease and become lower than the CCC. This would allow particles to be released causing bentonite loss. The rate of leaching of the ions from porewater will therefore influence the erosion rate.

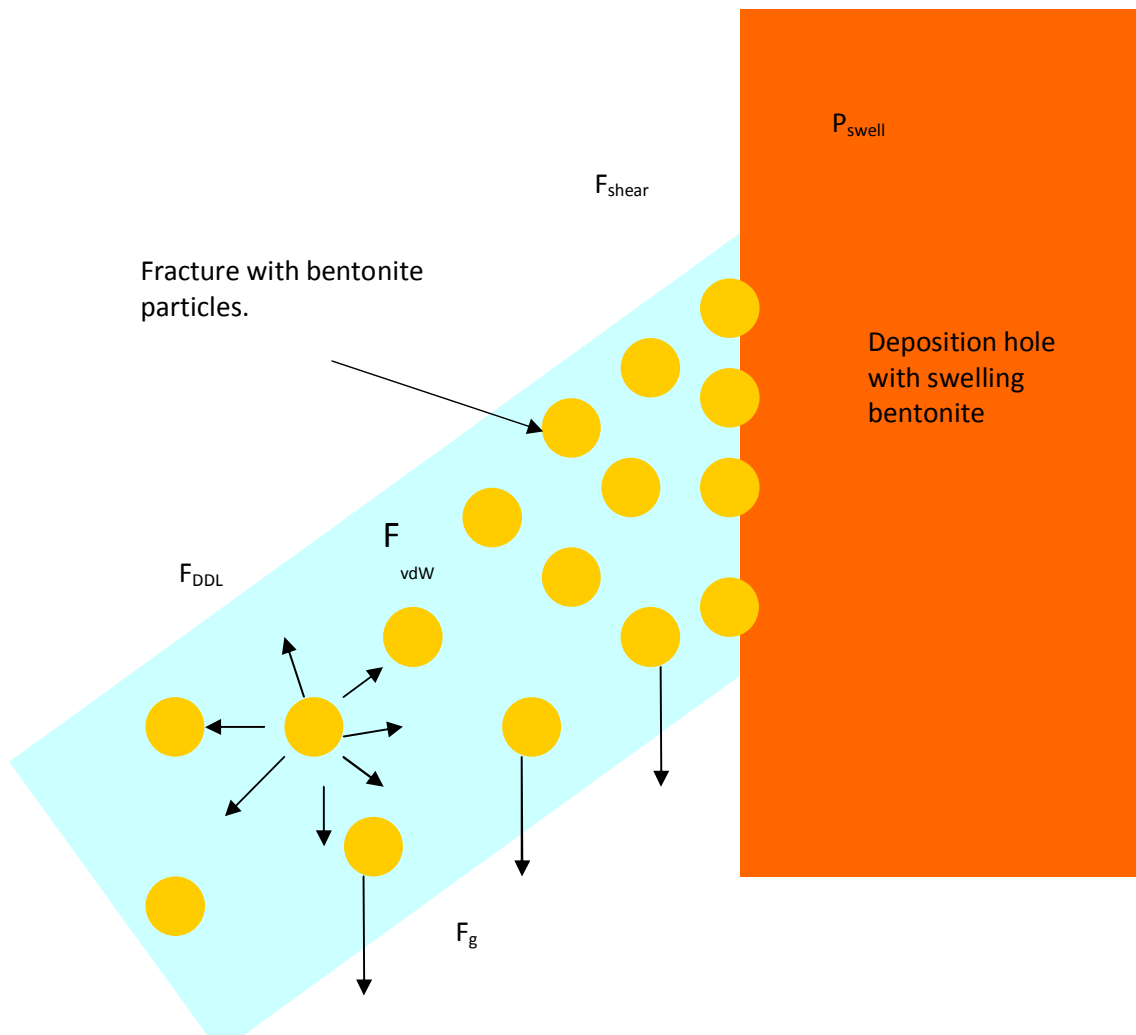


Figure 3.3. Schematic of forces acting on the bentonite in a deposition hole and fracture.

When the water composition in the buffer is below the CCC and when the water seeping in the fractures also is below the CCC the gel is always expansive and its rate of expansion will not be limited by the rate of leaching of CCC determining ions. The rate of expansion will then only be limited by the friction forces between the water and the particles in the gel/sol. In clays that contain non-smectite particles, these may conceivably also slow down expansion.

The rate of expansion would gradually slow down for two reasons. The expansion rate slows down inversely proportional to the square root of time because the water that intrudes into the gel has further and further to travel as the gel expands further into the fracture. Another reason is that should there be a noticeable loss of swelling pressure in the buffer due to loss of clay, the rate also slows down.

A further factor comes into play in practice. The commercial bentonites contain accessory minerals in addition to the smectite particles. This detritus material can be thought of as very fine sand. These particles are also influenced by the DDL forces that the smectite particles exert on them. Because of their different electrical charge properties they in general do not repel each other or the fracture walls as strongly as the smectite particles do. It is envisaged that as the smectite particles move into the fracture they will push the small sand particles in the same direction. Where the gel has expanded so much that it forms a sol, i.e. where the individual smectite particles no longer have strong repulsion forces between them and move essentially randomly and independently of each other propelled by thermal forces (Brownian diffusion), they no longer push or carry the "large" sand particles with them. These are left behind and could gradually build up a porous sand bed in the fractures. The smectite particles then have to move through the sand bed

to reach the mobile water. As more smectite is lost, the sand bed keeps increasing in size and is compressed by the smectite particles wanting to pass. The transport of the smectite particles will gradually slow down and may even totally stop when the sand bed is compressed and forms pores smaller than the smectite particles. This is called straining. The particle size distribution of the detritus material should be such that it overlaps with that of the smectite particles for the straining to be effective. Filtering and straining in short, a few mm depth bed formed under laboratory conditions, has been shown to effectively stop smectite penetration (Richards and Neretnieks 2010).

However, it remains to be shown that such filters will form by themselves in fractures and that they will be effective.

Even if the sand bed does not fully strain the smectite particles, it will slow down particle movement as well as the exchange of solutes between the seeping groundwater and the water in the bentonite. The longer the sand region is the longer distance ions and smectite have to diffuse, which limits the rate of mass transfer. The loss of CCC determining ions will slow down and may eventually become the rate-determining step for the colloid formation.

Figure 3.4 illustrates the expansion of the gel in a fracture, the formation of the sand bed and the transport of solutes and colloids through it. Here only the case when the water is below the CCC in the region around the gel/water interface is considered although it may be above the CCC further into the gel in the fracture. DDL forces expand the bentonite into the fracture. The fracture is slanting and gravity will therefore pull back upward expanding particles but pull them downwards into the water at the lower end of the intersection with the deposition hole. The sand particles are left behind when the gel turns to a sol and form a porous bed through which the smectite particles have to pass. This slows down the flux of the smectite particles. In addition, the sand and the gel will slow down the diffusion of ions from the pore water in the gel as the particles form a diffusion barrier. The sand will be pushed outward in the fracture by the swelling gel but will be restrained by friction. The particle size distribution in relation to the fracture aperture distribution will determine how far the particles can migrate before clogging the fracture. The particle size distribution of the detritus material in the commercial MX-80 bentonite overlaps that of fracture apertures and straining and clogging is expected to be potentially important mechanisms that can decrease or even stop erosion.

The thicker the sand bed becomes the more difficult it will be for it to move further out into the fracture. It is also expected that a sand bed will form in the deposition hole at the mouth of the fracture. This sand bed will be compressed and compacted by the swelling clay. The sand bed at the mouth of the fracture as well as in the fracture itself will grow with time but the rate of growth will decrease as less and less smectite particles can negotiate paths through the narrow pores of the bed.

In fractures with downward facing component, the sand particles can be pulled downward by gravity contributing to the loss of such particles. Hypothetically the whole downward facing fracture could be filled with such sedimenting sand particles if straining has not set a limit beforehand. The water flowrate will slow down in the fracture now filled with particles and its carrying capacity of smectite particle will decrease.

The solubilised smectite particles that reach the outer rim of the sand bed will diffuse into the boundary layer of the seeping water. During a given time they move a short distance into the seeping water. When the water has passed the deposition hole it has picked up a limited amount of colloids. This can be thought of as a resistance to colloid transfer to the seeping water. However, at the downward sloping part of the fracture, gravitation helps to pull the sol particles down into the water. At the lower end of the fracture, the rate of loss of smectite is therefore faster than at the upper parts.

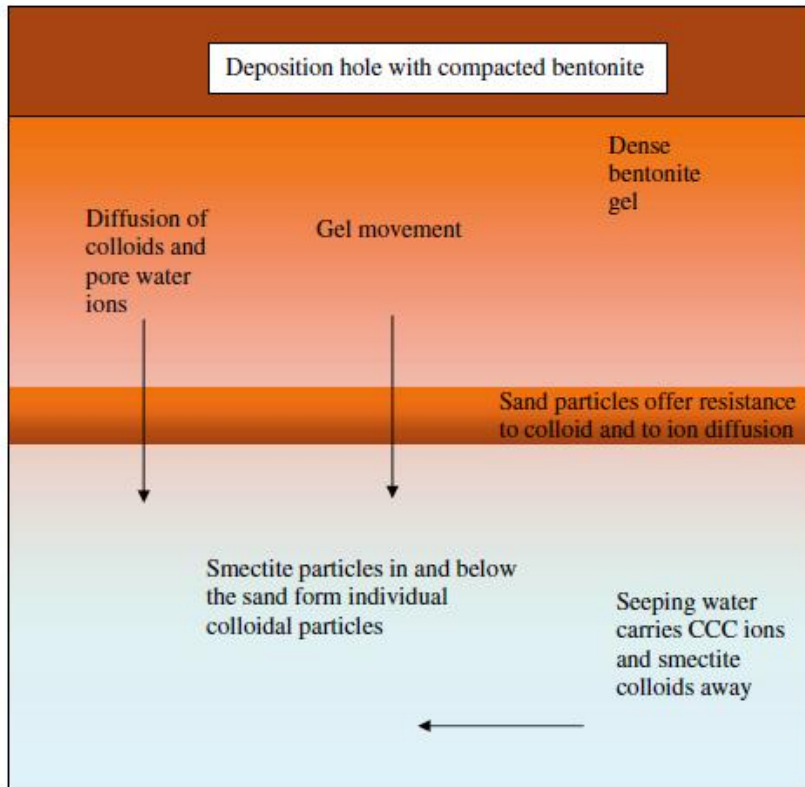


Figure 3.4. Bentonite gel expands downwards from the deposition hole into and in a fracture. Smectite colloids are released from the gel, move through the sand bed and are carried away by the seeping water.

3.1.4 Viscosity of smectite gel/sol

Broad overviews of rheological behaviour of bentonite/smectite suspensions can be found in Luckham and Rossi (1999), Bergaya et al (2006), and references therein. Barnes (1997) gives an overview of thixotropy. Measurements of shear stress-shear rate relations of purified and homoionic bentonite suspensions are reported in Chen et al (1990), Penner and Lagaly (2001), Adachi et al. (1998), Brandenburg and Lagaly (1988), Benna et al. (1999), Bekkour et al. (2005), Galindo-Rosales and Rubio-Hernández. (2006), Duran et al. (2000), Malfoy et al. (2007). Rheological properties of natural clays containing other mineral particles are reported in Christidis (1998), Christidis et al. (2006), Kelessidis et al. (2007). Methods used to determine layer charge and layer charge distributions are found in Frey and Lagaly (1979), Christidis (2008). Electroviscous effects are discussed by van der Ven (2001), and Rubio-Hernandez et al (2004).

These papers describe forces involved, shapes, sizes and structures of individual smectite sheets, cause of fixed and variable electric charges on the particle surfaces, influence of pH and ionic strength of the solution, association of individual particles in agglomerates of different sizes and shapes, impact of inorganic counterions in ion exchange positions of sorption and influence of non-ionic surfactants and polymers etc. Pseudoplastic effects and Bingham behaviour are described and analysed as well as causes for thixotropy and other nonlinear effects. The rheological behaviour of such suspensions is very complex and not understood in all details. Nevertheless, there are some effects that are generally agreed on qualitatively and sometimes also quantitatively.

Due to its direct influence on the electroviscous effect and the thickness of stacks, layer charge and charge heterogeneity is expected to strongly affect the rheological properties of smectite suspensions. This includes aspects of charge magnitude and charge localization (i.e. octahedral vs. tetrahedral) as well as the possibility of order or disorder in e.g. Mg-distribution, which influences octahedral charge (Christidis et al. 2006).

At high compaction the thin flat sheets must be aligned essentially parallel in stacks or quasi-crystals with very little space between the sheets. The distance between sheets in the stacks can be as low as 0.3 to 0.5 nm in “dry” clay when exposed to air with normal humidity (Push and Young 2006, Bergaya et al 2006). When compacted, the number of sheets in a stack is expected to be several hundred so that the stacks have approximately the same size in all directions at high compactions so that they can arrange themselves in a dense formation, avoiding large voids between the stacks. This is necessary in order to be able to compress the clay to porosities down to 0.3 to 0.4 without breaking or deforming the sheets too much. Such low porosities are readily obtained in the highly compacted bentonite blocks to be used as backfill in the repository. In water, the clay swells and the stacks distance themselves from each other and expand the distance between the sheets. The stacks also break up in thinner stacks and can break up into individual sheets, given favourable chemical conditions. The latter is observed for clays rich in sodium in the ion exchange positions and when the water has low salinity and not much divalent ions such as calcium and magnesium. In calcium rich clays and in waters with higher ionic strengths the sheets do not separate as readily and stacks or quasi-crystals of 5 to 15 or more sheets remain as coherent particles even when the clay has stopped swelling. Sodium rich clays behave very differently from calcium rich clays at lower solid volume fractions.

The movement of the individual particles is affected by the presence of neighbours as long as they do not have space enough to rotate freely. Rotation is a rather rapid process compared to other processes to be considered for the gel/sol behaviour (McBride and Baveye 2002). Onsager (1949) introduced the concept of co-volume where the basic idea is that the particles have volume in which to rotate freely without touching neighbouring spheres at low volume fractions. At higher volume fractions the rotation is hindered and this strongly influences the behaviour of the gel/sol.

The co-volume plays a central role in the model for the viscosity of dilute gel/sols. It is illustrated in Figure 3.5 below. The idea is that a fluid that contains spherical particles will be more viscous than the fluid itself

and that it can be described by the Einstein relation, at least at low volume fractions (Hiemenz 1986, Bird et al. 2002).

$$\eta = \eta_w (1 + 2.5\phi_{spheres}) \quad (1)$$

For higher volume fractions higher order terms could be added.

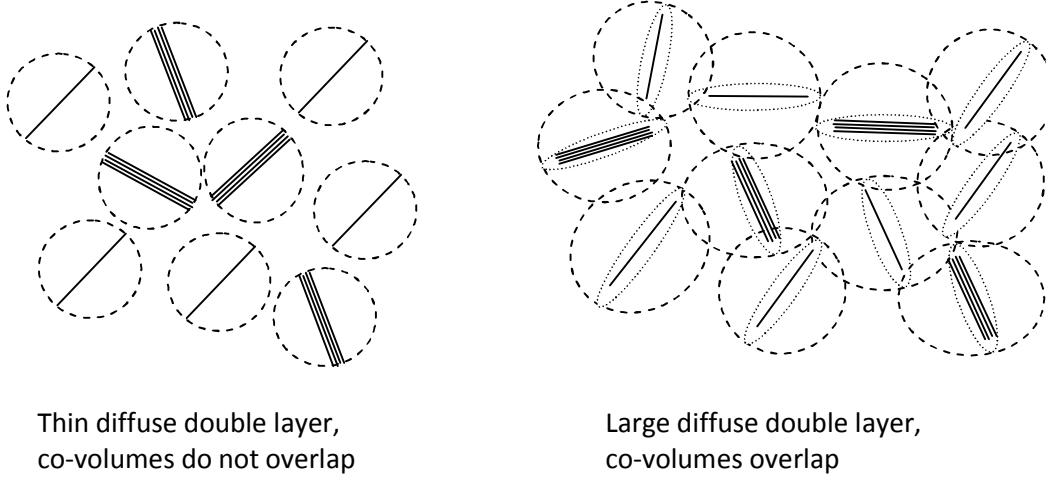


Figure 3.5. Illustration of co-volume with and without impact of diffuse layer for a given volume fraction ϕ . The extent of the diffuse layer is shown as dotted oval in the right figure.

For coin-like particles the co-volume is the volume of a sphere, which the particle could rotate in. Liu (2011) extended the idea by to the radius of the coin adding some fraction m of the thickness of the diffuse double layer. This is illustrated in Figure 3.5. The diffuse layer extends further in low ionic strength waters and the viscosity will therefore tend to increase with decreasing ionic strength.

Liu (2011) used data for sodium bentonites and purified smectites from different sources and was able to fit the following expression to the data.

$$\frac{\eta}{\eta_w} = 1 + 1.022\phi_{cov}^\kappa + 1.358(\phi_{cov}^\kappa)^3 \quad (2)$$

where

$$V_{cov} = \frac{\pi(l_s + 2m\kappa^{-1})^3}{6} \quad (3)$$

The Debye length is

$$\kappa^{-1} = \sqrt{\frac{\epsilon_0 \epsilon RT}{2IF^2}} \quad (4)$$

$$\phi_{cov}^\kappa = \frac{V_{cov}}{V_p} \phi = \frac{2}{3} \frac{(l_s + 2m\kappa^{-1})^3}{l_s^2 \delta_s n} \phi \quad (5)$$

The number m of Debye lengths to add to the radius of the sheet was found to be 1 and the particle radius $l_s = 220$ nm in the fitting of all the data shown in Figure 3.6. The data cover actual volume fractions ϕ up to nearly 0.9 %.

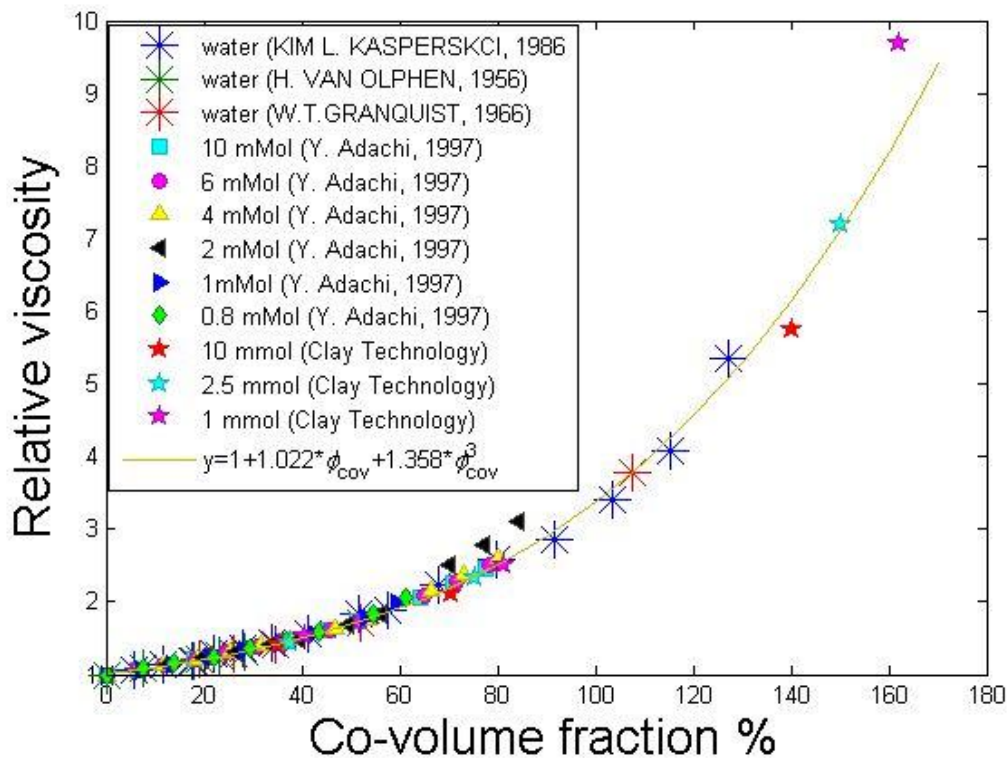


Figure 3.6. Relative viscosity as a function of co-volume fraction from different sources.

Viscosity data for sodium smectites for higher volume fractions exist. Birgersson et al. (2009) show strong non-Newtonian behaviour and the data cannot be used for this model. The little information found for calcium bentonites could also not be used.

There is a need to develop better understanding and models for calcium bentonites and for higher volume fractions because gel/sol viscosity models are an essential part of erosion modelling.

3.1.5 Forces on and between smectite particles

3.1.5.1 Overview

To be able to understand and simulate the behaviour of a compacted bentonite in a deposition hole, swelling under water uptake, expansion out in the fracture as the gel becomes looser and release of colloidal particle to the seeping water we need to account for the forces that govern this process.

The underlying conceptual model is that the gel consists of thin smectite sheets aligned in parallel until the gel is so dilute that they can rotate freely. Gravity and buoyancy forces on the particles and attractive van der Waals forces as well as repulsive double layer forces between particles act to move the particles when these forces do not balance. The movement is restrained by friction against the water in which they move.

The force balance is used to set up the equation of continuity to define the change in space and time of the expanding gel. The double layer repulsive forces are based on a solution of the Poisson-Boltzmann equation. A new analytical solution was devised by Liu and Neretnieks (2007), which is valid over the whole range of solid volume fraction in the gel of interest here, namely from $0 < \phi < 0.7$. The particle friction is based on the Stokes-Einstein relation for individual particles in the dilute gel and on a modified Kozeny-Carman

relation for the dense gel. Recently, also a correlation for the friction as related directly to the force balance model was devised, which is an alternative to the Kozeny-Carman relation, Liu (2010).

A special bonus with the dynamic force balance model is that was successfully used to predict the range of CCC for sodium as well as calcium bentonites, much better than the conventional DLVO theory does, Liu et al. (2009b).

The dynamic model has been successfully tested against accurate measurements of sodium smectite tablet expansion, starting from a dry density of 1800 kg/m^3 expanding upwards in test tubes. It has also been attempted to use the model to simulate calcium bentonite expansion but although modelling results qualitatively and semi-quantitatively agree reasonably well with the experiments there are differences that makes the prediction of calcium bentonite swelling less reliable. Also the present model cannot predict the formation and properties of stacks that form in calcium systems.

The dynamic force balance model makes up a central part of our larger model used for bentonite erosion simulations.

3.1.5.2 Forces involved

The particles in a gel or sol will be acted on by a number of different forces. The action of these forces on the particles determines the expansion and contraction of the gel and the formation of sols. The understanding and modelling of these forces form the basis for the modelling. The following forces are considered here,

- F_g Gravity and buoyant force
- F_μ Forces due to changes in chemical potential in a concentration gradient
- F_{vdW} van der Waals attractive forces
- F_{DDL} Repulsive forces due to the presence of electrical charges in and on the smectite particles, so called diffuse double layer forces
- F_η Friction forces on the particles if they move due to imbalance of the previous forces

The sum of these forces shall be zero

$$F_\eta = -(F_\mu + F_g + F_{DDL} + F_{vdW}) \quad (6)$$

Friction forces on the particles and gravity

Gravity acts on a particle, pulling it downward. The force on the particle is proportional to its buoyant mass and is

$$F_g = V_p (\rho_p - \rho_w) g_c \quad (7)$$

The friction force on a spherical particle can for laminar flow conditions be expressed by (Bird et al. 2002)

$$F_\eta = u_p f_{fr} = 3\pi\eta_w d_p u_p \quad (8)$$

η_w is the viscosity of water and d_p is the particle diameter.

For particles with other shapes, this can be generalized to

$$f_{fr} = 6\pi\eta_w r_{eqv} \quad (9)$$

For large thin coin-like particles with diameter d_{coin} it is

$$r_{eqv} = \frac{d_{coin}}{\pi} \quad (10)$$

The above relations can be used to describe the friction factor in suspensions. Denser gels need to be treated differently and the concept of a porous bed in which the water moves in the narrow spaces between the particles used. For laminar flow friction is proportional to the velocity in the pores and to the magnitude of the surface the water “rubs” against.

The friction force in a porous medium such as a bed of small particles can be estimated from a relation attributed to Kozeny and Carman called the Kozeny-Carman or the Blake-Kozeny relation, when the flow is laminar, which is valid for Reynolds number $Re < 1$. (Bird et al 2002, p 191)

The idea behind this relation is that the space between the particles forms conduits in which the fluid flows and the pressure drop in the conduits can be described in the same way as in a tube. When the “tubes” in the bed are the conduits between the particles the pressure drop in the bed can be assigned to each particle and a friction factor defined for the particle in the bed.

$$f_{fr} = \frac{1-\phi}{\phi} \frac{\eta_w}{k} V_p \quad (11)$$

The permeability k for the bed could be taken from the Kozeny-Carman relation. However for the bentonite beds a modification of that relation gives better agreement over the whole range of experimental conditions. Permeability data for MX-80 and similar bentonites (Karnland et al. 2006) were used to obtain the dependence of k on ϕ . It was found, with the method detailed in (Liu 2010, 2011), that the permeability of natural MX-80 is very different from that of sodium exchanged bentonite. It can be well described over a wide range of solution concentrations by, for purified and sodium exchanged smectite with $k_0=182$

$$k = \frac{1}{k_0 a_R^2} \frac{(1-\phi)^3}{\phi^3} \quad (12)$$

for natural MX-80 bentonite where $k_0=0.6$

$$k = \frac{1}{k_0 a_R^2} \frac{(1-\phi)^6}{\phi^2} \quad (13)$$

If one uses the Kozeny-Carman relation or similar ones to describe the permeability, the friction factor as given in Equation (11) would go to zero when the volume fraction approaches 0. No theoretical model describing the transition has been found and it was chosen to add the friction factors for a single particle to that obtained for the bed. This gives a smooth transition in the intermediate range. Petsev et al. (1993) also tested the Kozeny-Carman equation over a wide range of volume fractions and arrived at similar conclusion.

$$f_{fr} = f_{fr,particle} + f_{fr,bed} \quad (14)$$

Chemical potential and particle “diffusion”

All particles in the water including the water molecules are subject to random movements. This causes them to spread out and eventually attain a constant concentration everywhere provided no other forces are present. This can also be formulated as a force acting on the particles. It is only active as long as there is concentration gradient of particles.

$$F_\mu = -k_B T \frac{d\phi}{dz} \frac{1}{\phi} \quad (15)$$

van der Waals forces

van der Waals forces between two parallel particles are described by Equation (16) (Evans and Wennerström 1999). The vdW force is always attractive.

$$F_{vdW} = A_p \frac{A_H}{6\pi} \left[\frac{1}{h^3} - \frac{2}{(h+\delta_p)^3} + \frac{1}{(h+2\delta_p)^3} \right] \quad (16)$$

Diffuse double layer forces

These are the most important forces that cause the expansion and solubilisation of the smectite particles in low ionic strength water and therefore described in somewhat more detail.

The smectite particles have a negative charge mainly due to isomorphous substitution in the crystal lattice of silicon (Si) for aluminium (Al) and aluminium for divalent atoms such as iron (Fe) and magnesium (Mg). This leads to a net negative charge on the order of one meq/g. One can also view this as an equivalent mass of 1000 g/eq. This means that the smectite has a considerable permanent charge, which must be neutralized by attachment of charge compensating ions. These are commonly sodium (Na), potassium (K), calcium (Ca) and magnesium (Mg) ions. In addition to the fixed charges, the surface of the smectite particle, which is made up of silica, can hydrolyse and attach water to form S=OH groups on the surface. S= stands for surface here. These groups can detach protons (H⁺) when pH of the water is high to form negatively charged surface groups S=O⁻ or attach protons in low pH waters to form positive groups S=OH₂⁺. At the edges also the alumina layer sandwiched between the two silica layers can be hydrolysed and protonated or de-protonated. In circum neutral water most of these surface groups are neutral in low ionic strength waters with negligible amounts of specifically sorbing ions and do not add or detract much to the surface charge.

When the smectite particles are wetted, the ions dissolve in the water but stay very near to the surface in what is called a diffuse double layer. This is illustrated in 3.7. Anions are largely depleted in the diffuse layer.

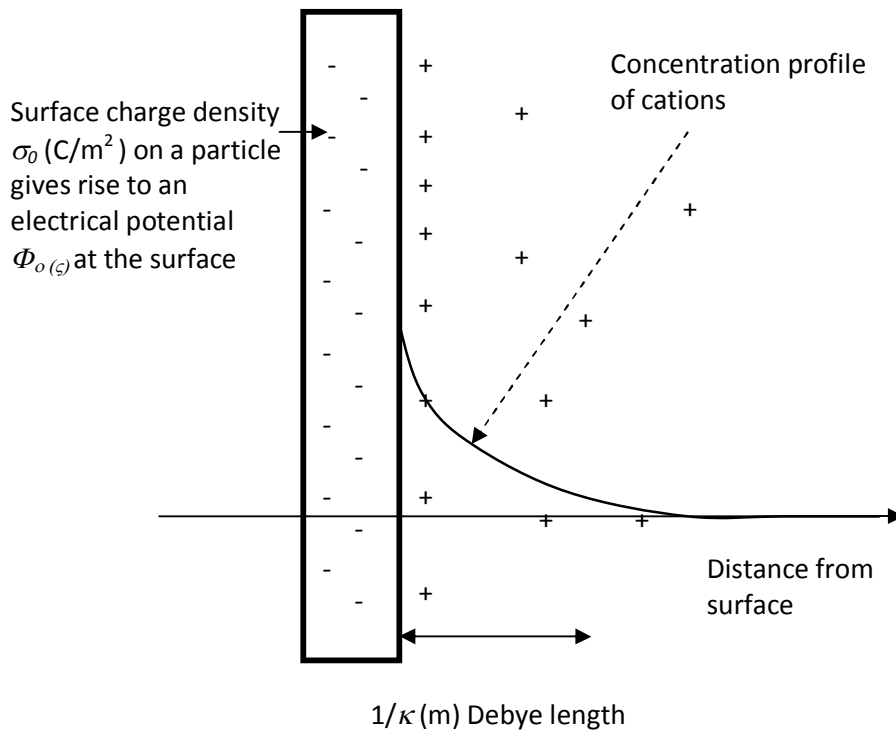


Figure 3.7. Negative charges in a smectite particle generate a diffuse layer of counter ions in the water

A measure of the distance can be assessed from the Debye length $1/\kappa$ Equation(4). Figure 3.8 shows $1/\kappa$, for mono- and divalent ions as a function of ion concentration. In very low ionic strength water the Debye length can reach 1000 nm for monovalent ions and 500 nm for divalent ions. At high ion concentration the diffuse layer will be compressed. In the concentration range 0.01 to 0.1 mM the Debye length is of the same magnitude as the size (side length) of the smectite particles. This is of some interest because at higher ion concentration, diffuse layer forces between particles will have a smaller influence and the particles can orient themselves more freely.

Debye length $1/\kappa$, m

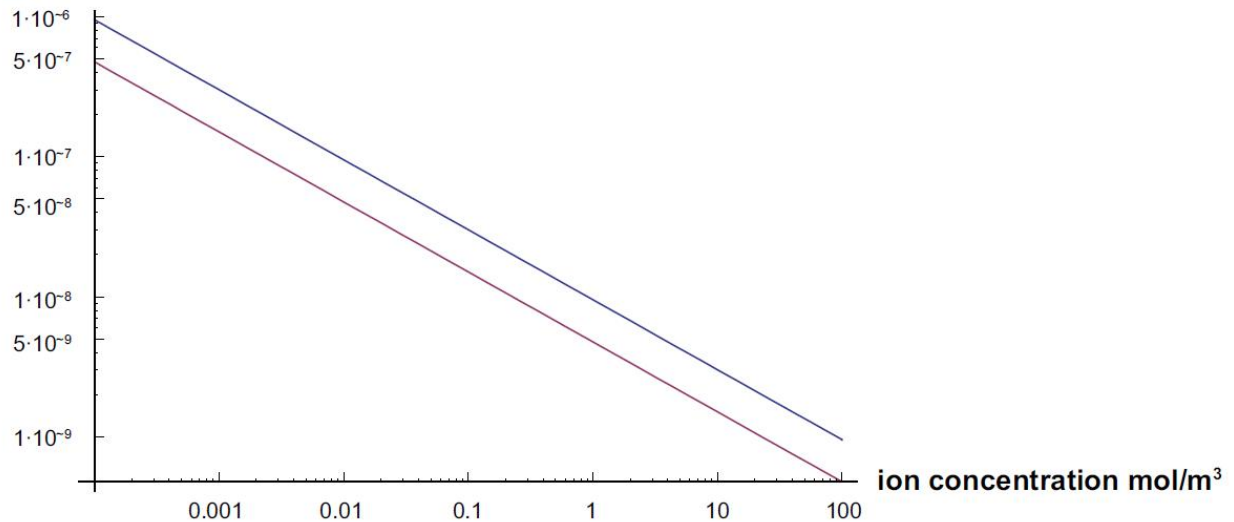


Figure 3.8. Debye length as function of ion concentration for $z=1$, upper curve and $z=2$ lower curve.

If smectite particles come so near that the diffuse layers overlap considerably strong repulsive forces develop. This is the reason for the strong swelling pressures found in wet compact bentonite.

The pressure repelling the particles is described by the Poisson-Boltzmann equations. This has been experimentally verified for monovalent ion dominated water but break down when divalent ions dominate, when the particles are close and when the surface charge density is high. Under such conditions the DDL forces can become strongly attractive. This is deemed to be the reason behind the stack formation in calcium dominated systems. It is not understood why the stacks still repel each other as strongly as they do and why calcium dominated smectite have swelling pressures comparable to sodium-dominated systems at high to intermediate compaction.

Exact analytical solutions to Poisson-Boltzmann equations have been published for special cases but are very complex and computationally unwieldy. Several approximate expressions, which are useful for different situations are also available. Evans and Wennerström (1999) or Lyklema (2005) present extensive discussions on the different approximate expressions. The main differences between the different models are that they apply for constant potential or constant charge and that they are valid in either high or low particle distances. Liu and Neretnieks (2007) devised a model for constant charge. It compares well with the exact solution of the Poisson-Boltzmann equations for the full range of concentrations and particle distances of interest for this study. It has the advantage over the exact solution that it is considerable faster to evaluate and is readily twice differentiable, which is needed in the dynamic model used to simulate the expansion and erosion.

The reader is referred to the paper by Liu and Neretnieks (2007) for the full equations. Here for illustration purposes one simple equation is shown, which is a good approximation for the DDL forces for low surface charge or low surface potential and for not very small particle distances. Equation (17) shows the pressure between two flat particles as a function of the Debye length, surface potential and distance between

particles. It illustrates that the repulsion force drops off exponentially with particle distance and that the Debye length plays an important role.

$$P_{DDC} = 64cRT \cdot \text{Tanh}^2\left(\frac{yd \cdot z}{4}\right) e^{-h\kappa} \quad (17)$$

and yd is the dimensionless surface potential.

$$yd = \frac{\Phi_0 F}{RT} \quad (18)$$

Equation (17) cannot be used for small $h\kappa$ because when the particles approach the assumption of constant potential is no longer valid for the constant charge particles of interest here.

Figure 3.9 is based on the solution of the Poisson-Boltzmann equation by Liu and Neretnieks (2007) and it shows the pressure between the particles as function of distance for $z=1$ and $\sigma_0=-0.131 \text{ C/m}^2$ for $c=0.1$ to 50 mol/m^3 . It is seen that for low ionic strengths the disjoining pressure can extend to distances larger than the sheet diameter. At small distances very large repulsion forces are predicted. Note, in addition, that the straight portions of the curves agree with what Equation (17) predicts.

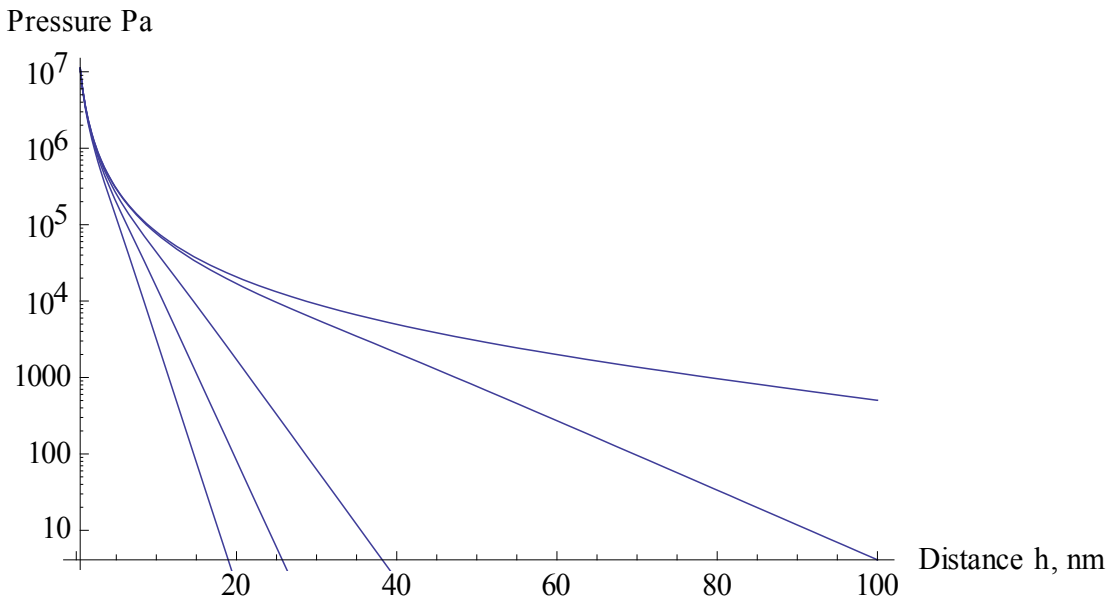


Figure 3.9. Disjoining pressure as a function of distance between particles for monovalent ions. Curves from left to right $c=50, 25, 10, 1$ and 0.1 mol/m^3 .

3.1.5.3 Balancing the forces

Figure 3.10 shows the forces acting between and on the particles. The conceptual picture is that the sheets within a stack must be aligned in parallel at higher densities. Stacks can have any orientation. Balancing all forces against the friction force that will restrain its movement and will determine at what velocity a particle moves in the relation to the water.

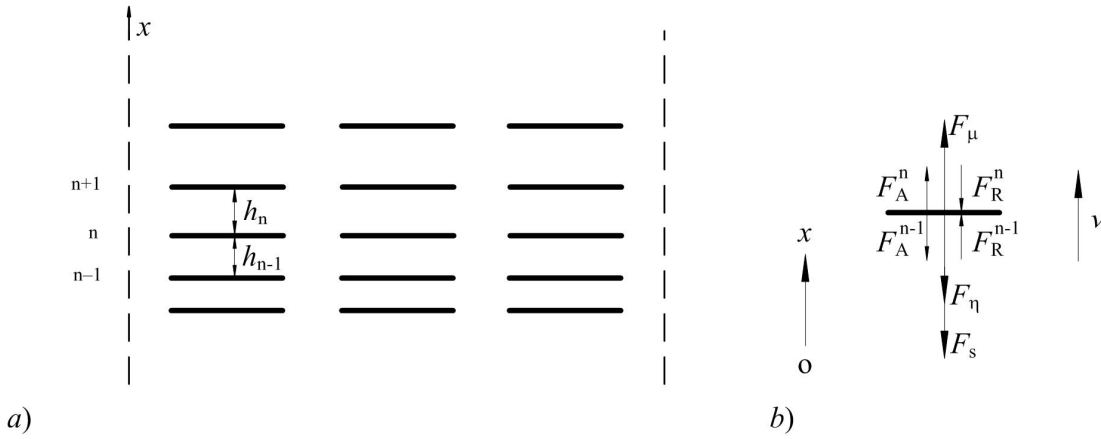


Figure 3.10. Sketch of a) the conceptual model and b) the forces acting on an arbitrary particle in a suspension.

Summation of all forces and after some rearrangement and manipulation the flux J of particles relative the water is found to be.

$$J = \frac{F_g \phi}{f_{fr}} - \frac{k_B T}{f_{fr}} \frac{d\phi}{dx} + \frac{d}{dh} (F_{vdW} - F_{DDL}) \frac{(h + \delta_p)^2}{f_{fr}} \frac{d\phi}{dx} \quad (19)$$

or

$$J = \frac{F_g \phi}{f_{fr}} - \frac{\chi}{f_{fr}} \frac{d\phi}{dx} \quad (20)$$

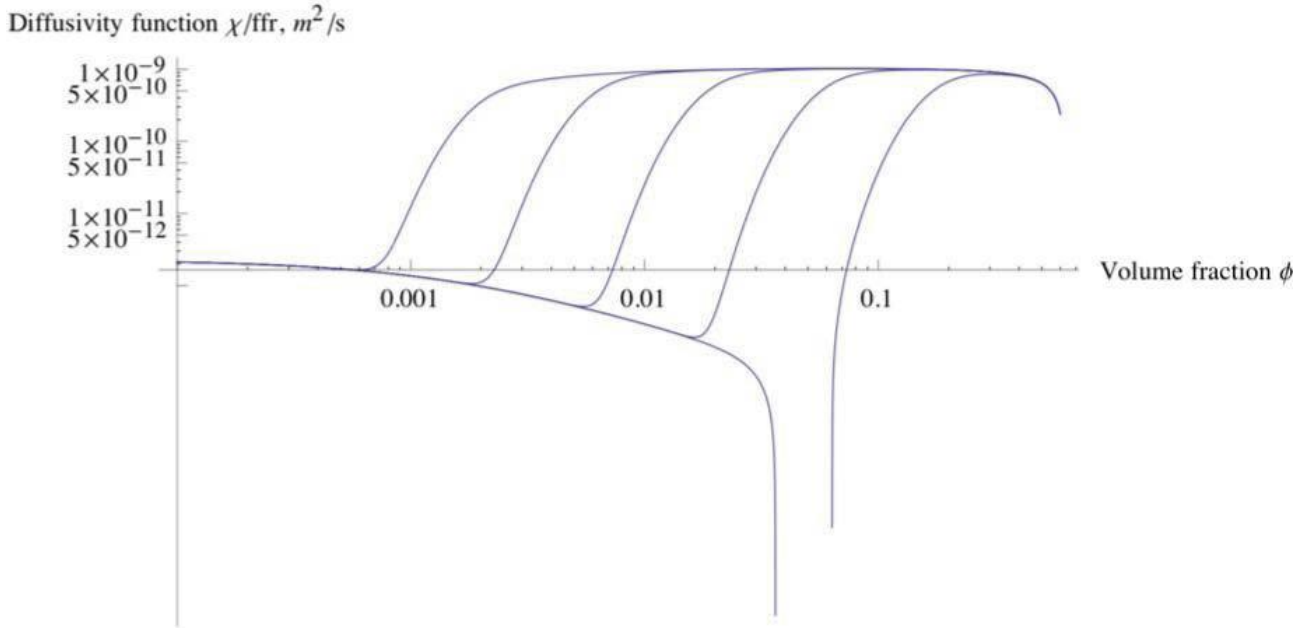
with

$$\chi = k_B T + \frac{d}{dh} (F_{vdW} - F_{DDL}) (h + \delta_p)^2 = k_B T + \frac{d}{dh} (F_{vdW} - F_{DDL}) \left(\frac{\delta_p \phi_{max}}{\phi} \right)^2 \quad (21)$$

The entity $\frac{\chi}{f_{fr}}$ may be thought of as a diffusion coefficient, which can vary strongly with particle concentration ϕ and water chemistry. This entity is called the diffusivity function,

$$D_F = \frac{\chi}{f_{fr}} \quad (22)$$

For very low particle concentrations where neither vdW nor DDL forces are important and where gravity plays no role Equation (20) simplifies to the expression for Fick's first law.



3. 11. Diffusivity function for smectite 300 nm diameter sheets for monovalent ions. The curves from left to right are for 0.1, 1, 10, 50 and 100 mM ion for $z=1$, $\lambda_p=10^{-9}$ m and $\sigma_0=-0.131$ C/m²

Figure 3.11 shows the diffusivity function for different ion concentrations. To the left the diffusivity is that of individual particles due to Brownian motion and is about 10^{-13} m²/s. For 0.01 mM this applies up to $\phi=0.0006$. At higher particle concentrations the DDL forces start to become noticeable and DF increases rapidly. It levels off at about 10^{-9} m²/s for all ion concentrations. At an ion concentration just above 50 mM the DDL forces become weaker than the vdW forces and D_F becomes negative at ϕ around 0.05. This means that the particles will move closer to each other instead of diffusing away from each other and will stabilize at a distance where the sum of the interaction energies is minimum. The ion concentration at which this happens is the CCC. This is another way of understanding the CCC phenomenon and predicts the CCC much better than the DLVO theory does for sodium as well as for calcium (Liu et al. 2009b). The CCC depends not only on the surface charge density and the charge of the counterion but also on the thickness of the particles and of the surface area of the particles. For monovalent ions the CCC is predicted to lie between 40 and 100 mM for thin (1.2 nm thick) particles larger than 10000 (nm)². The CCC increases with decreasing particle size.

With divalent counterions the CCC is predicted to lie between 0.7 and 2 mM for 15 nm (8 sheets at a distance of 1 nm in a stack) thick particles larger than 10000 (nm)² and half these values for twice as thick particles. This agrees well with observed values. The traditional DLVO theory predicts about *two orders of magnitude larger* CCC for flat particles.

The CCC can be derived directly from the force function for the ion concentration at which $\chi=0$. Liu et al. (2009b) present some simple relations that can be used to assess the CCC.

3.1.6 Dynamic model for gel/sol expansion

The equation of continuity is used to describe the evolution in time and space of a smectite gel. It states that what is transported in minus what is transport out of a control volume will accumulate in the volume or be depleted from the volume if more goes out than in. In the limit when the volume is made infinitely small the continuity equation can be written as

$$\frac{\partial \phi}{\partial t} = -\frac{\partial J}{\partial x} \quad (23)$$

With the flux J inserted, and setting $f = f_{fr}/(1-\phi)$, it becomes

$$\frac{\partial \phi}{\partial t} = -F_s \frac{\partial}{\partial x} \left(\frac{\phi}{f} \right) + \frac{\partial}{\partial x} \left(\frac{\chi}{f} \frac{\partial \phi}{\partial x} \right) \quad (24)$$

The first term shows the accumulation per time unit, the second is movement due to body forces. The third term accounts for in- and out-flux due to diffusion and forces between the particles. The model is also applicable for other one-dimensional problems, such as colloidal sedimentation in a gravity field. The equation can be readily extended to three dimensions. A similar idea has been proposed by Petsev et al. (1993) for expansion of a bed consisting of spherical particles.

Equation (24) can be used to describe the dynamic evolution of the colloidal system in time and space. It is the central result of the expansion model. A number of examples using the model to validate it against experiments are presented in Liu et al. (2009a, b) and Neretnieks et al. (2009).

3.1.6.1 *Mathematical model for bentonite expansion in a fracture and release of colloids*

The dynamic model has been used to simulate the expansion and erosion of bentonite in a fracture that intersects a deposition hole filled with compacted bentonite. The water has a much lower sodium concentration than the pore water in the compacted bentonite and sodium diffuses outward in the gel in the fracture and is carried away by the seeping water. The volume fraction of smectite in the gel/sol and therefore the gel viscosity decreases continuously outward in the fracture. The gel/sol will therefore flow in the fracture but very slowly nearest to the deposition hole and with increasing velocity further from the hole as both the sodium concentration and the volume fraction of smectite decreases.

To model these processes the dynamic model must be coupled to and solved simultaneously with the sodium diffusion model, the model for viscosity and the model that describes the flow of gel/sol and water in the fracture. The problem is 2-dimensional.

The advection-diffusion equation is used to model sodium migration in the fluid. Only the cation needs to be modelled as the anion transport is obtained from the charge balance. Sodium is used as the migrating cation as this is the dominating species in the systems considered. The advection-diffusion equation is given by

$$\frac{\partial c}{\partial t} = -\bar{u} \nabla c + \nabla \cdot (D \nabla c) \quad (25)$$

The left hand side term is the accumulation term. The first term on the right hand side denotes the advective transport and the second the diffusive transport.

The equation describing the mass balance for smectite in the system is similar to the advection-diffusion equation. It is the same as the dynamic model Equation (24) but with an added term that accounts for the flow of the gel, the third term. It is written to be useful also for 2 and 3 dimensional systems.

$$\frac{\partial \phi}{\partial t} = \bar{F}_s \nabla \left(\frac{\phi}{f} \right) - \bar{u} \nabla \phi + \nabla \cdot \left(\frac{\chi}{f} \nabla \phi \right) \quad (26)$$

Here $\bar{f} = \bar{f}_{fr}/(1-\phi)$ to account for the movement of the smectite relative to fixed coordinates in contrast to Equation (24) where the smectite flux is relative to the water, which moves in the other direction.

3.1.6.2 An example of simulation results

In the simulations the fracture size is chosen so large that the presence of the deposition hole and expanding smectites has a minor impact on the water velocity at large distances. In this case it is at least 10 m times 5 m with a cylindrical deposition hole 1.75 m in diameter. Larger fracture sizes were used for lower water velocities. The numerical calculations using the cylindrical geometry are somewhat unstable due, possibly, to the existence of a stagnation point in the velocity field. Also the equations are quite non-linear in some regions and rapid changes of several variables over short distances occur, which also contributes the numerical difficulties. The penetration distance into the fracture increases with time but stabilizes eventually. Only the steady state results are presented below.

The smectite volume fraction and the velocity field are shown in Figure 3.12 for the large water velocity 315 m/yr. Figure 3.13 shows the same results for a fracture with a ten times smaller water velocity.

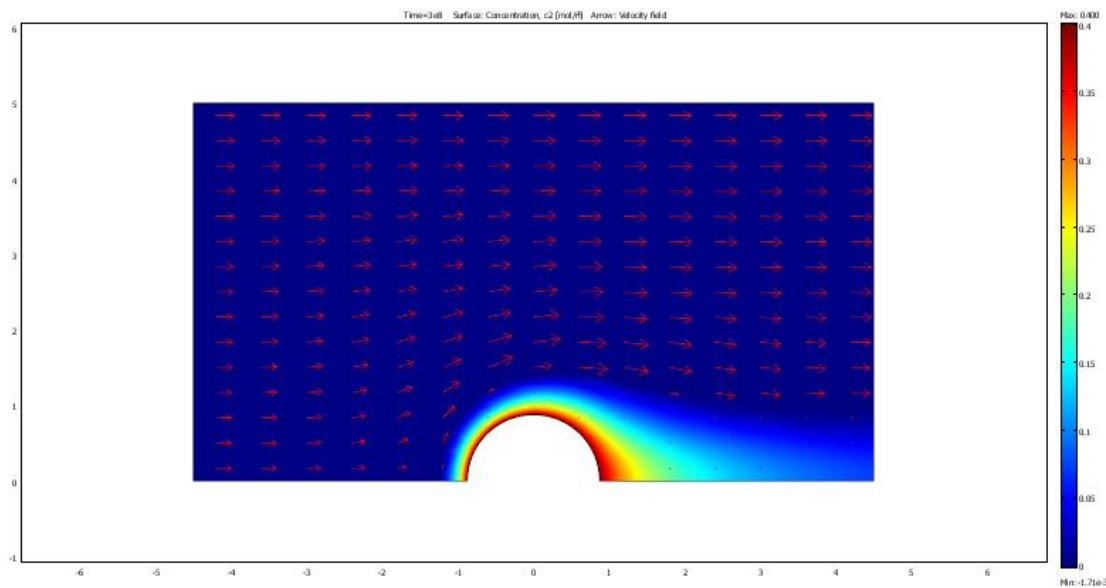


Figure 3.12. Smectite volume fraction distribution and velocity field (as arrows) for an approaching water velocity in the fracture of 315 m/yr.

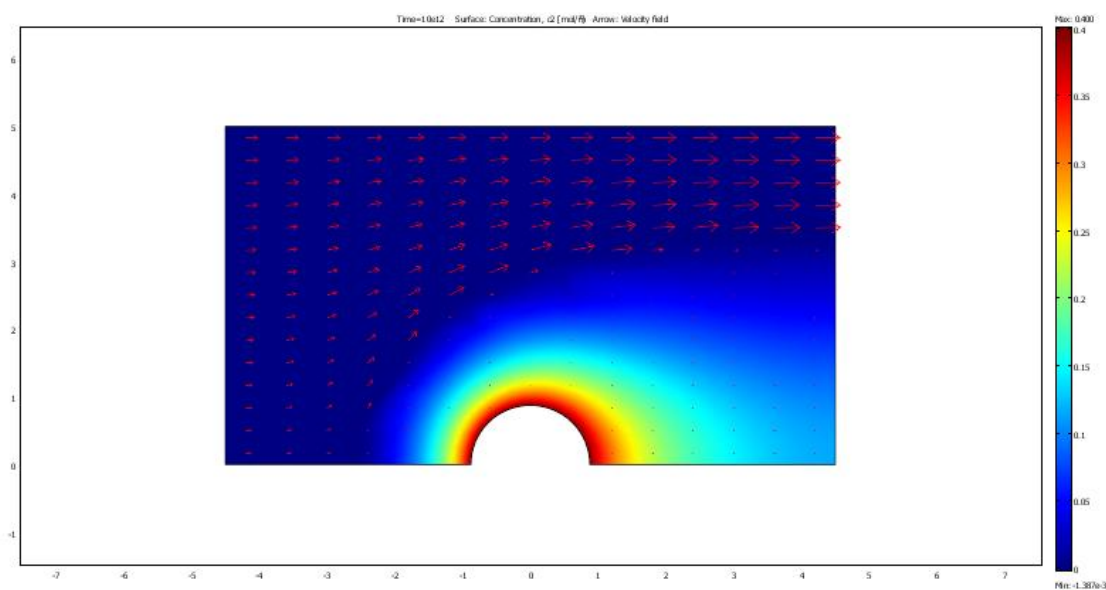


Figure 3.13. Smectite volume fraction distribution and velocity field (as arrows) for a water velocity of 31.5 m/yr.

The water velocity has a strong impact on the resulting erosion rates. This is seen in Figure 3.14.

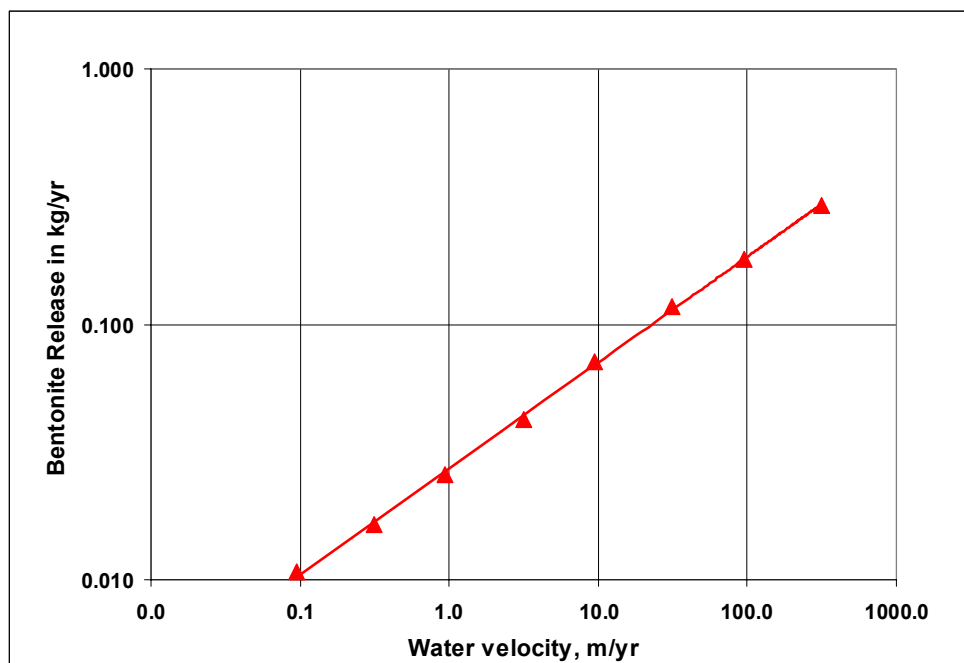


Figure 3.14. Smectite release for different fracture transmissivities.

At low water velocities the penetration depth is larger than at high velocities as seen in Figure 3.14 above. It is conceivable that under other conditions penetration depth could be larger. Then also the amount of smectite residing in the fracture must be considered, as this also would constitute a loss of mass from the deposition hole.

3.2 Erosion of bentonite - modifications of baseline model by VTT

3.2.1 Introduction

VTT's modelling concept has this far been parallel to KTH's approach. VTT has, however, made a family of model implementations, which are called by general name BESW. During the process on doing those models and trying to apply them to experimental data, some general observations have been done that are listed in the following.

- Initial model includes basically two forces, expanding force and internal friction, but this leads to certain contradictions
 - o conceptual: it is tempting to assume that the swelling material is somehow interacting with fracture surfaces
 - o experimental: in small scale experiments montmorillonite is observed to have limited and stable extrusion depth at high salinity, while the extrusion depth is getting larger and erosion starts to appear by decreasing salinity below some critical salinity
 - o PA related: by applying the initial type of modelling over the whole period from installation to post glacial conditions, the extrusion depth will be even 100 metres due diffusion type of advancing
- Differences between laboratory conditions and the full scale
 - o in full scale, the salinity diffusion out of the bentonite is an essential part of the model, while in laboratory conditions constant salinity experiments may be carried out for purified montmorillonite, making the modelling a bit easier
 - o in laboratory scale, on the other hand, it is difficult to start by initially fully saturated and aged samples, and therefore the laboratory scale modelling needs additional modelling efforts for saturation during erosion

No effort to include the abovementioned topics into VTT's modelling has been done yet.

3.2.2 The modifications implemented

In order to enhance numerical computation in COMSOL Multiphysics, some functional dependencies have been simplified. All simplifications are based on relatively simple analytical relations, for which first order partial derivatives are also available.

The needed processes and their related parameters are shown in Table 1. Note that while volume fraction affects all three transport parameters and concentration two, the pressure has no effect via transport parameters.

Table 1. The processes, variables and transport parameters applied in BESW-model. The units, mutual dependencies and variable names applied in COMSOL are also shown.

Process	Name	Unit	Transport parameter	Name	Unit	Dep. on c	Dep. on ϕ	Dep. on p
Diffusion of sodium, concentration	c	mol/m ³	Diffusion coefficient	D	m ² /s	no	yes	no
Transport smectite, volume fraction	ϕ	-	Diffusion coefficient	D_F	m ² /s	yes	yes	no
Darcy flow, pressure	p	Pa	Viscosity	η_{rel}	1	yes	yes	no

For relative viscosity Neretnieks et al. (2010) apply equation 2. Therefore, the relative viscosity fully written out in case of particle diameter $D_p = 250$ nm and thickness $\delta_p = 1$ nm

$$\eta_{\text{rel}} = 1 + k_5 \left(1 + \sqrt{\frac{k_7}{c}}\right)^3 \phi + k_6 \left(1 + \sqrt{\frac{k_7}{c}}\right)^9 \phi^3 = 1 + k_5 \beta(c)^3 \phi + k_6 \beta(c)^9 \phi^3 \quad (27)$$

in which

$$\beta(c) = 1 + \sqrt{\frac{k_7}{c}}$$

$$k_5 = a_1 \frac{2D_p}{3\delta_p} = 170.33$$

$$k_6 = a_3 \left(\frac{2D_p}{3\delta_p}\right)^3 = 6.287 \times 10^6$$

$$k_7 = \frac{2\varepsilon\varepsilon_0 RT}{D_p^2 F^2} = 5.922 \times 10^{-3} \frac{\text{mol}}{\text{m}^3}$$

The conceptual thinking for further simplifications is sketched in Figure 3.15, where the diffusivity is shown as a function of ϕ at four salinity levels. The high diffusivity value D_F^h is reached with all salinity values when ϕ is high enough (> 0.1). At low ϕ values the behaviour looks more complicated due to the minimum value of diffusivity at salinity dependent ϕ values.

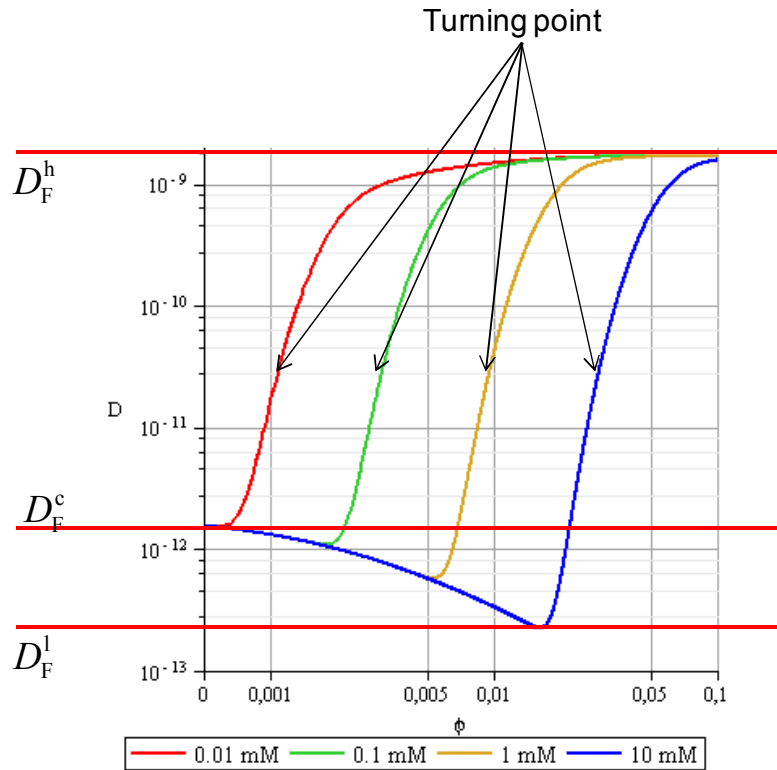


Figure 3.15. Diffusivity of smectite as a function of volume fraction of smectite (ϕ) and salinity (ionic strength). At the four ionic strengths shown, the diffusivity curve has a distinct turning point, before which diffusivity is low and which it high. The location of turning points depends on salinity.

It is though logical and even physically reasonable to consider two distinct diffusivity functions: one for colloidal diffusion ($D_F^c(c)$) and one for gel like smectite. Therefore, a function α is sought for the following fit of smectite diffusivity.

$$D_F(\phi, c) = D_F^l \cdot \left(\frac{D_F^h}{D_F^l} \right)^{\alpha(\phi, \phi(c))} + D_F^c(c) \quad (28)$$

The function α has been chosen to be (see parameter values in Table 2)

$$\alpha(\phi, c) = \frac{1}{1 + \left(\frac{\ln \phi}{\ln A + b \ln c} \right)^n} \quad (29)$$

Table 2. Parameter for α function.

Parameter	Value	Unit
n	16	-
A	0.009± 3.90E-005	-
b	0.492± 0.0020	-
D_F^h	1.6e-9	m ² /s
D_F^l	1e-13	m ² /s
D_F^c	1.9e-12	m ² /s

Full diffusivity function becomes then as in equation 30.

$$D_F(\phi, c) = D_F^l \cdot \left(\frac{D_F^h}{D_F^l} \right)^{\left[1 + \left(\frac{\ln \phi}{\ln(Ac^b)} \right)^n \right]^{-1}} + D_F^c = D_F^l \cdot \left(\frac{D_F^h}{D_F^l} \right)^{\left[1 + \left(\frac{\ln \phi}{\ln A + b \ln c} \right)^n \right]^{-1}} + D_F^c \quad (30)$$

When using α function the full diffusivity function becomes as in equation 31.

$$D_F(\phi, c) = D_F^l \cdot \left(\frac{D_F^h}{D_F^l} \right)^{\alpha(\phi, c)} + D_F^c = D_F^l \cdot \left(\frac{D_F^h}{D_F^l} \right)^{\alpha(\phi, c)} + D_F^c \quad (31)$$

In order to make the model hierarchy clearer, a flowchart of the workflow presented as Figure 3.16 has been produced. The following notation is used.

- Direct application of the implementation - BESW on COMSOL Multiphysics: functions in data form, BESW_D, or symbolic approximation, BESW_S - of Neretnieks' et al. (2009) model.
- Approximate calculation method developed at VTT, BESW_A.

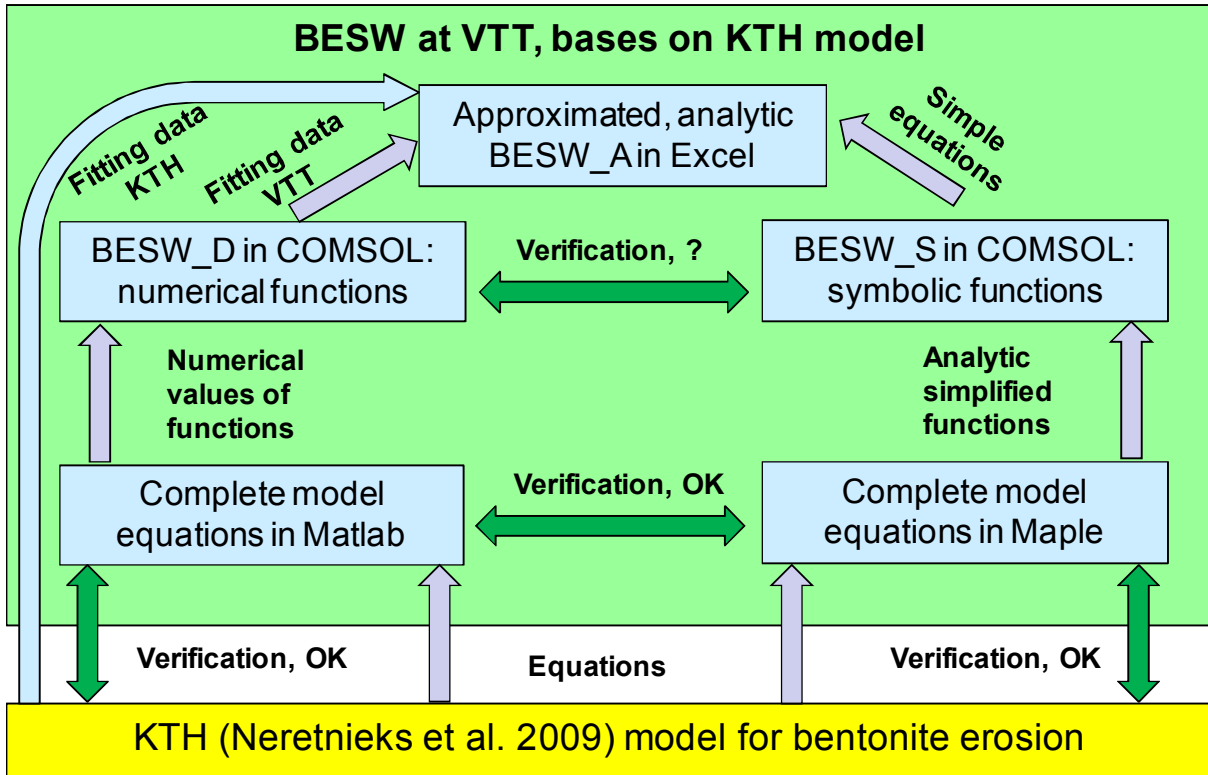


Figure 3.16. Coupling between original Neretnieks' model and VTT's different implementations. Note, that BESW_A model applied in this work is fitted to original KTH data.

The BESW model is described detail forthcoming Posiva reports. Therefore, it was chosen to apply numerical functions in COMSOL Multiphysics instead of implementing the functions directly. In this approach the values of functions are given over a mesh and COMSOL interpolates and extrapolates the function values needed (BESW_D implementation). All functions were tested in Matlab before applying them into COMSOL. All functions were implemented onto symbolic mathematics program Maple, too.

Finally, BESW_A is an extreme simplification in which model geometry (R_1 is the source term radius in cylindrical geometry), extrusion depth (L) and groundwater flow velocity (v) are coupled by the simple formula presented in equation 32.

$$v = A \left(\frac{\phi_1}{\phi_0} \right)^2 \frac{1}{R_2 \left[\ln \left(\frac{R_2}{R_1} \right) \right]^2} = A \left(\frac{\phi_1}{\phi_0} \right)^2 \frac{1}{(R_1 + L) \left[\ln \left(\frac{R_1 + L}{R_1} \right) \right]^2} \quad (32)$$

where A is a fitting parameter (applied either for experimental data or results from more complicated calculations) and ϕ_0 is the reference volume fraction i.e. that used in model calculations to be fitted.

3.3 Transport of bentonite colloids

3.3.1 Conceptual models

3.3.1.1 Interactions with the stationary phase

Most of the model studies found in the literature have assumed equilibrium interactions between the colloidal phase and the contaminant in the dissolved phase (Chrysikopoulos and Abdel-Salam, 1997) analogous to the model developed by Corapcioglu and co-workers (Corapcioglu and Jiang, 1993). Another step in the model development was to implement the influence of reversible and irreversible radionuclide

sorption processes showing that slow desorption kinetics of the contaminant from the colloid is an essential prerequisite in order for nanoparticle-facilitated contaminant transport to become significant (Artinger et al., 2002; Bekhit and Hassan, 2007; Bouby et al., 2010; Contardi et al., 2001; Ibaraki and Sudicky, 1995). Colloids/ nanoparticles interaction with the stationary phase (porous media, fracture surface) is classically implemented via correlation equations to calculate the theoretical single-collector efficiencies (based on the filter theory), either classical (Rajagopalan and Tien, 1976) or with the more recently published Tufenkji and Elimelech correlation (Tufenkji and Elimelech, 2004a; Tufenkji and Elimelech, 2004b; Tufenkji and Elimelech, 2005), where the overall reaction can be formulated as first-order kinetics.

3.3.1.2 Heterogeneity of the domain

Recent advances included inter alia the implementation of physical and chemical heterogeneity (Bekhit and Hassan, 2005; Severino et al., 2007) which remains a key challenge in describing nanoparticle transport and retention (McCarthy and McKay, 2004). In the EU IP-FUNMIG project a twofold approach was used to tackle the issue of colloid transport, namely (a) programming an object oriented code (CHEPROO, CHEmical PRocesses Object-Oriented) that is capable to simulate complex hydrobiogeochemical processes and is open to include more complex chemical systems as e.g. solid solutions, nanoparticle transport without loss in the handling of simple problems (Bea *et al.*, 2009) and (b) to characterize and monitor by integrating the analytical tools available within the FUNMIG consortium to a maximum extend the heterogeneity of natural systems observed in nanoparticle transport experiments. The methods included *inter alia* μ CT (computer tomography) to characterize the fracture geometry (Enzmann and Kersten, 2006), C-14 PMMA impregnation (Kelokaski et al., 2006; Leskinen et al., 2007; Sardini et al., 2006; Voutilainen et al., 2009) and application of positron-emission-tomography (PET) to direct visualisation of the solute transport and nanoparticle transport in this natural rock fracture (Kulenkampff *et al.*, 2008). Based on the geometrical data available a comparison between experimental determined colloid breakthrough curves and computational fluid dynamics (CFD) modelling of colloid migration in a stationary flow field using this real 3D geometrical information was made (Huber et al., 2012). Simplified fracture geometry assumption as e.g. parallel plate models using the average fracture aperture were not capable to simulate appropriate the colloid breakthrough behaviour.

3.3.2 Numerical implementation

The implementation of a nanoparticle transport code was not completed within FUNMIG, but recently a Lagrangian particle tracking model (PTM) was proposed for predicting colloid/nanoparticle transport near a rough surface by embedding protruding spherical asperities in a planar surface (Kemps and Bhattacharjee, 2009). In summary, the model results show that asperities protruding from the planar surface can act as additional collectors, either directly or indirectly through changing the flow field. All the observations made in this study indicate that physical surface heterogeneity has a far reaching influence on particle deposition and it is important to accurately determine the flowfield near roughness features in nanoparticle deposition models in order to reliably predict deposition efficiencies or deposit morphologies.

Notation

a_R	Specific area of particles, area/particle volume
A_H	Hamaker constant
A_p	Particle surface area one side
c	Concentration of ions
d_{coin}	Coin-like particle diameter
d_p	Particle diameter
D_F	Diffusivity function for particles
D	Diffusivity in water
f_{fr}	Friction factor based on velocity difference between water and particles
F	Faraday constant
F_{DDL}	Diffuse layer force between particles
F_g	Buoyancy force on particle
F_{vdW}	van der Waal's force between particles
F_η	Friction force on particle
F_μ	Force on particle due to chemical potential
g_c	Gravitation constant
h	Distance between sheets
I	Ionic strength
J	Flux (flowrate/cross section area)
k	Permeability
k_0	Kozeny's constant
k_B	Boltzmann constant
l_s	Lateral extent of sheet
n	Number of sheets in a stack
P_{DDL}	Pressure due to double layer forces
r_{eqv}	Equivalent radius of particles
R	Gas constant
T	Absolute temperature
u	Velocity
u_p	Particle velocity
V_{cov}	Co-volume for particle
V_p	Volume of particle
x	coordinate
yd	Dimensionless surface potential
z	Valence of ions, coordinate
δ_s	Sheet thickness
ε	Relative permeability
ε_0	Permittivity in vacuum
η	Viscosity
η_w	Viscosity of water
κ	Reciprocal Debye length
ρ_s	Density of smectite
ρ_w	Density of water
σ_0	Surface charge density
ϕ	Volume fraction of solids (1- ε) in gel/sol
ϕ_{cov}^K	Co-volume fraction including effects of electrical double layer extension
Φ_0	Surface electrical potential

References

- Abend S., Lagaly G., 2000, Sol–gel transitions of sodium montmorillonite dispersions, *Applied Clay Science*, 16, 201–227
- Adachi Y., Nakaishi K., Tamaki M., 1998, Viscosity of a dilute suspension of sodium montmorillonite in a electrostatically stable condition, *J. Colloid and Interface Science* 198, 100–105
- Artinger, R., Schuessler, W., Schäfer, T., Kim, J.I., 2002. A kinetic study of Am(III)/humic colloid interactions. *Environmental Science & Technology*, 36(20): 4358-4363.
- Barnes H.A., 1997, Thixotropy – a review, *J. Non-Newtonian Fluid Mech.*, 70, 1-33
- Bea, S.A., Carrera, J., Ayora, C., Batlle, F., Saaltink, M.W., 2009. CHEPROO: A Fortran 90 object-oriented module to solve chemical processes in Earth Science models. *Computers & Geosciences*, 35(6): 1098-1112.
- Bekhit, H.M., Hassan, A.E., 2005. Stochastic modeling of colloid-contaminant transport in physically and geochemically heterogeneous porous media. *Water Resources Research*, 41(2).
- Bekhit, H.M., Hassan, A.E., 2007. Subsurface contaminant transport in the presence of colloids: Effect of nonlinear and nonequilibrium interactions. *Water Resources Research*, 43(8).
- Bekkour K., Leyama M., Benchabane A.I., Scrivener O., 2005, Time-dependent rheological behaviour of bentonite suspensions: An experimental study, *J. Rheol.* 49(6), 1329-1345
- Benna, M., Kbir-Ariguib, N., Magnin, A., Bergaya, F., 1999, Effect of pH on rheological properties of purified sodium bentonite suspensions. *J. Colloid Interface Sci.* 218, 442–455.
- Bergaya F., Theng B.K.G., Lagaly G., Ed., Elsevier, 2006, *Handbook of Clay Science*
- Bird R.B., Stewart W.E., Lightfoot E.N., 2002, *Transport Phenomena*, Wiley,
- Birgersson M., Börgesson L., Hedström M., Karnland O., Nilsson U., 2009, Bentonite erosion, Final Report from Clay Technology, Swedish Nuclear Fuel and Waste management Co., SKB TR-09-34
- Boisson J.Y., 1989, Study on the Possibilities by Flowing Ground Waters on Bentonite Plugs Expanded from Borehole into Fractures, *Proc. NEA/CEC Workshop Sealing of Radioactive Waste Repositories*
- Brandenburg U., Lagaly G., 1988, Rheological Properties of sodium montmorillonite dispersions, *Applied Clay Science*, 3, 263-279
- Bouby, M. et al., 2010. Colloid/ Nanoparticle formation and mobility in the context of deep geological nuclear waste disposal (Project KOLLORADO-1; Final report), Forschungszentrum Karlsruhe, Karlsruhe.
- Chen, J.S., Cushman, J.H., Low, P.F., 1990. Rheological behavior of Na-montmorillonite suspensions at low electrolyte concentration. *Clays Clay Miner.* 38, 57–62.
- Christidis G.E., 1998, Physical and chemical properties of some bentonite deposits of Kimolos Island, Greece, *Applied Clay Science*, 13, 79-98
- Christidis G.E., Blum A.E., Eberl D.D., 2006, Influence of layer charge and charge distribution of smectites on the flow behaviour and swelling of bentonites, *Applied Clay Science* 34, 125–138
- Christidis G.E., 2008, Validity of the structural formula method for layer charge determination of smectites, A re-evaluation of published data, *Applied Clay Science*, 42, 1-7
- Chrysikopoulos, C.V., Abdel-Salam, A., 1997. Modeling colloid transport and deposition in saturated fractures. *Colloids and Surfaces A*, 121: 189 - 202.
- Contardi, J.S., Turner, D.R., Ahn, T.M., 2001. Modeling colloid transport for performance assessment. *Journal of Contaminant Hydrology*, 47(2-4): 323-333.

- Corapcioglu, M.Y., Jiang, S., 1993. Colloid-Facilitated Groundwater Contaminant Transport. *Water Resources Research*, 29, 7: 2215 - 2226.
- Duran, J.D.G., Ramos-Tejeda, M.M., Arroyo, F.J., Gonzáles-Caballero, F., 2000. Rheological and electrokinetic properties of sodium montmorillonite suspensions: I. Rheological properties and interparticle energy of interaction. *J. Colloid Interface Sci.* 229, 107–117.
- Enzmann, F., Kersten, M., 2006. X-ray computed micro tomography (μ -XRT) results of a granitic drill core. In: Reiller, P., Buckau, G., Kienzler, B., Duro, L. (Eds.), 1st Annual workshop Proceedings of IP FUNMIG, report CEA R-6122. Commissariat a l'energie atomique (CEA), Gif sur Yvette (France), pp. 211-215.
- Evans D.F., Wennerstöm H., 1999, *The colloidal domain*, Wiley
- Frey E., Lagaly G., 1979, Selective coagulation in mixed colloidal suspensions, *Journal of Colloid and Interface Science*, 70 (1)
- Galindo-Rosales F.J., Rubio-Hernández F.J., 2006, Structural breakdown and build-up in bentonite dispersions, *Applied Clay Science*, 33, 109-115
- Grindrod, P., Peletier, M., Takase, H., 1999. Mechanical interaction between swelling compacted clay and fractured rock, and the leaching of clay colloids. *Eng. Geol.* 54, 159–165.
- Hiemenz P.C., 1986, *Principles of Colloid and Surface Chemistry*, Marcel Dekker, NY
- Huber, F. et al., 2012. Natural micro-scale heterogeneity induced solute and nanoparticle retardation in fractured crystalline rock. *Journal of Contaminant Hydrology*, 133: 40-52.
- Ibaraki, M., Sudicky, E.A., 1995. Colloid-facilitated contaminant transport in discretely fractured porous media .1. Numerical formulation and sensitivity analysis. *Water Resources Research*, 31(12): 2945-2960.
- Kanno T., and. Wakamatsu, H., 1991, Experimental Study on Bentonite Gel Migration from a Deposition Hole, Proc. 3rd Int. Conf. Nuclear Fuel Reprocessing and Waste Management (RECOD '91).
- Kanno, T., Matsumoto, K., Sugino, H., 1999, Evaluation of extrusion and erosion of bentonite buffer, Proc. 7th Int. Conf. on Radioactive Waste Management and Environmental Remediation (ICEM '99).
- Karnland O., Olsson S., Nilsson U. 2006, Mineralogy and sealing properties of various bentonites and smectite-rich clay materials, Swedish Nuclear Fuel and Waste management Co., SKB Technical Report, TR-06-30
- Kelessidis V.C., Tsamantaki C., Dalamarinis P., 2007, Effect of pH and electrolyte on the rheology of aqueous Wyoming bentonite dispersions, *Applied Clay Science*, 38, 86-96
- Kelokaski, M., Siitari-Kauppi, M., Sardini, P., Mori, A., Hellmuth, K.H., 2006. Characterisation of pore space geometry by C-14-PMMA impregnation - development work for in situ studies. *Journal of Geochemical Exploration*, 90(1-2): 45-52.
- Kemps, J.A.L., Bhattacharjee, S., 2009. Particle Tracking Model for Colloid Transport near Planar Surfaces Covered with Spherical Asperities. *Langmuir*, 25(12): 6887-6897.
- Kulenkampff, J., Grundig, M., Richter, M., Enzmann, F., 2008. Evaluation of positron-emission-tomography for visualisation of migration processes in geomaterials. *Physics and Chemistry of the Earth*, 33(14-16): 937-942.
- Kurosawa, S., Kato, H., Ueta, S., Yokoyama, K., Fujihara, H., 1999, Erosion properties and dispersion-flocculation behavior of bentonite particles. *Mater. Res. Soc. Symp. Proc.* 556, 679–686.
- Leskinen, A. et al., 2007. Determination of granites' mineral specific porosities by PMMA method and FESEM/EDAX. *Scientific Basis for Nuclear Waste Management XXX*, 985: 599-604.

- Liu, L., 2010. Permeability and expansibility of sodium bentonite in dilute solutions. *Colloids Surf. A: Physicochem. Eng. Aspects* 358 (1–3), 68–78.
- Liu L., 2010. Permeability and expansibility of sodium bentonite in dilute solutions. *Colloids Surf. A: Physicochem. Eng. Aspects* 358 (1–3), 68–78.
- Liu L., 2011, A model for the viscosity of dilute smectite gels, *Physics and chemistry of the earth*, 36, p 1792-1798
- Liu J., Neretnieks I., 2006, Physical and chemical stability of the bentonite buffer, Swedish Nuclear Fuel and Waste management Co., SKB report R-06-103
- Liu, L.; Neretnieks, I., 2007, Homo-interaction between Parallel Plates at Constant Charge, *Colloids Surf. A: Physicochem. Eng. Aspects* 2008, 317, 636.
- Liu, L., Moreno, L., Neretnieks, I., 2009a. A Dynamic force balance model for colloidal expansion and its DLVO-based application. *Langmuir* 25 (2), 679–687.
- Liu, L., Moreno, L., Neretnieks, I., 2009b. A novel approach to determine the critical coagulation concentration of a colloidal dispersion with plate-like particles. *Langmuir* 25 (2), 688–697.
- Luckham, P.F., Rossi, S., 1999. The colloidal and rheological properties of bentonite suspensions. *Adv. Colloid Interface Sci.* 82, 43–92.
- Lyklema, J., 2005, *Fundamentals of Interface and Colloid Science, Vol. IV: Particulate Colloids*, Elsevier
- McBride M.B., Baveye P., 2002, Division S-2-Particle interactions in colloidal systems, *Soil Sci. Am J.* 66, 1207-1217
- Malfoy C., Fontaine C., Pantet A., Monnet P., 2007, The effect of mineralogical and cationic heterogeneities on rheological properties of suspensions with Li-smectites, extracted from Volclay MX-80, *C. R. Geoscience*, 339, 960-969
- McCarthy, J.F., McKay, L.D., 2004. Colloid transport in the subsurface: past, present, and future challenges. *Vadose Zone Journal*, 3: 326-337.
- Moreno L., Neretnieks I., Liu L., 2010, modelling of bentonite erosion Swedish Nuclear Fuel and Waste management Co., SKB TR-10-64.
- Moreno L., Neretnieks I., Liu L., 2011, Erosion of sodium bentonite by flow and colloid diffusion, *Physics and chemistry of the earth*, 36, p 1600-1606
- Neretnieks, I., Liu, L., Moreno, L., 2009. Mechanisms and Models for Bentonite Erosion. Swedish Nuclear Fuel and Waste management Co., Swedish Nuclear Fuel and Waste management Co., SKB TR-09-35
- Onsager L., 1949, The effect of shape on the interaction of colloidal particles. *Ann. N.Y. Acad. Sci.* 51: 627-659
- Penner D., Lagaly G., 2001, Influence of anions on the rheological properties of clay mineral dispersions, *Applied Clay Science*, 131–142
- Petsev D.N., Starov, I.B. Ivanov, 1993, Concentrated dispersions of charged colloidal particles: sedimentation, ultrafiltration V.M. and diffusion, *Colloids and Surfaces A: Physicochemical and Engineering Aspect* 81, 65-81
- Pusch, R., 1983, *Stability of Bentonite Gels in Crystalline Rock — Physical Aspects*. SKBF/KBS TR-83-04. Swedish Nuclear Fuel and Waste Management Co., Stockholm.
- Pusch, R., 1999. *Clay Colloid Formation and Release from MX-80 Buffer*. Swedish Nuclear Fuel and Waste management Co., SKB TR-99-31. Swedish Nuclear Fuel and Waste Management Co., Stockholm.

- Pusch R., Young R.N., 2006, Microstructure of smectite clays and engineering performance, Taylor and Francis,
- Pusch R., 2007, Colloids formed from buffer clay- nature and physical stability, Report. Geodevelopment international AB, Ideon Science park. SE-22370 LUND, SWEDEN, 2007-03-22
- Rajagopalan, R., Tien, C., 1976. Trajectory analysis of deep-bed filtration with the sphere-in-cell porous media model. *Am. Inst. Chem. Eng. J. AIChE*, 22: 523-533.
- Richards T., Neretnieks I., 2010, Filtering of clay colloids in bentonite detritus material. *Chem. Eng. Technol.*, 33, No 8, 1303-1310
- Rubio-Hernández F.J., Carrique F., Ruiz-Reina E., 2004, The primary electroviscous effect in colloidal suspensions, *Advances in Colloidal and Interface Science*, 107, 51-60
- Sardini, P., Siitari-Kauppi, M., Beaufort, D., Hellmuth, K.H., 2006. On the connected porosity of mineral aggregates in crystalline rocks. *American Mineralogist*, 91(7): 1069-1080.
- Sen, T.K., Khilar, K.C., 2006. Review on subsurface colloids and colloid-associated contaminant transport in saturated porous media. *Advances in Colloid and Interface Science*, 119(2-3): 71-96.
- Severino, G., Cvetkovic, V., Coppola, A., 2007. Spatial moments for colloid-enhanced radionuclide transport in heterogeneous aquifers. *Advances in Water Resources*, 30(1): 101-112.
- Sjöblom, R., Kalbantner, P., Bjurström, H., Pusch, R., 1999. Application of the general microstructural model to erosion phenomena— Mechanisms for the chemical-hydrodynamic conversion of bentonite to a pumpable slurry in conjunction with retrieval. *Eng. Geol.* 54, 109–116
- Tanai, K., Matsumoto, K. 2007: A study on extrusion behavior of buffer material into fractures using X-ray CT method, *Proc. 3rd International Meeting on Clays in Natural & Engineered Barriers for Radioactive Waste Confinement*.
- Tufenkji, N., Elimelech, M., 2004a. Correlation equation for predicting single-collector efficiency in physicochemical filtration in saturated porous media. *Environmental Science & Technology*, 38(2): 529-536.
- Tufenkji, N., Elimelech, M., 2004b. Deviation from the classical colloid filtration theory in the presence of repulsive DLVO interactions. *Langmuir*, 20(25): 10818-10828.
- Tufenkji, N., Elimelech, M., 2005. Breakdown of colloid filtration theory: Role of the secondary energy minimum and surface charge heterogeneities. *Langmuir*, 21(3): 841-852.
- van de Ven T.G.M., 2001, Electroviscous phenomena in colloidal dispersions, *Chemical Engineering Science*, 56, 2947-2955
- van Olphen H., 1977, *An Introduction to Clay Colloid Chemistry: For Clay Technologists, Geologists, and Soil Scientists*, John Wiley and Sons: New York.
- Verbeke, J., Ahn, J., Chambré P. L., 1997, Long-Term Behaviour of Buffer Materials in Geologic Repositories for High-Level Wastes, Report University of California at Berkeley UCB-NE-4220 (1997).
- Voutilainen, M., Lamminmaki, S., Timonen, J., Siitari-Kauppi, M., Breitner, D., 2009. Physical Rock Matrix Characterization: Structural and Mineralogical Heterogeneities in Granite. *Scientific Basis for Nuclear Waste Management* xxxii, 1124: 555-560.